Original Paper

Cells Tissues Organs

Cells Tissues Organs 2007;185:285–307
DOI: 10.1159/000102176

Accepted after revision: January 25, 2007

Are Distributions of Secondary Osteon Variants Useful for Interpreting Load History in Mammalian Bones?

John G. Skedros[a, b] Scott M. Sorenson[b] Nathan H. Jenson[a]

[a]Department of Orthopaedic Surgery, University of Utah, and [b]Bone and Joint Research Laboratory, Department of Veteran's Affairs Medical Center, Salt Lake City, Utah, USA

Key Words
Osteon · Bone adaptation · Cement line · Strain mode · Load history

Abstract

Background/Aims: In cortical bone, basic multicellular units (BMUs) produce secondary osteons that mediate adaptations, including variations in their population densities and cross-sectional areas. Additional important BMU-related adaptations might include atypical secondary osteon morphologies (zoned, connected, drifting, elongated, multiple canal). These variants often reflect osteonal branching that enhances toughness by increasing interfacial (cement line) complexity. If these characteristics correlate with strain mode/magnitude-related parameters of habitual loading, then BMUs might produce adaptive differences in unexpected ways. ***Methods:*** We carried out examinations in bones loaded in habitual torsion (horse metacarpals) or bending: sheep, deer, elk, and horse calcanei, and horse radii. Atypical osteons were quantified in backscattered images from anterior, posterior, medial, and lateral cortices. Correlations were determined between atypical osteon densities, densities of all secondary osteons, and associations with habitual strain mode/magnitude or transcortical location. ***Results:*** Osteon variants were not consistently associated with 'tension', 'compression', or neutral axis ('shear') regions, even when considering densities or all secondary osteons, or only osteon variants associated with relatively increased interfacial complexity. Similarly, marrow- and strain-magnitude-related associations were not consistent. ***Conclusion:*** These data do not support the hypothesis that spatial variations in these osteon variants are useful for inferring a habitual bending or torsional load strain history.

Abbreviations used in this paper

BMU	basic multicellular unit
Cd	caudal
Cr	cranial
DED	drifting, elongated and doublet-connected osteons (in fig. 4C, D, H)
Dor	dorsal
En	endosteal aspect of the cortex
Lat	lateral
MC3	equine third metacarpal
Med	medial
Mi	middle aspect of the cortex
NREs	new remodeling events
OHI	osteon heterogeneity index
$OHI_{(A)}$	(TAO)/(On.N/T.Ar)
$OHI_{(DED)}$	osteon heterogeneity index in the DED group
On.Ar/T.Ar	fractional area of secondary osteonal bone × 100 (%, includes central canals in T.Ar)
On.N/T.Ar	secondary osteon population density per total (T) mm^2 area (Ar) (n/mm^2, includes central canals in T.Ar)
Pal	palmar
Pe	periosteal aspect of the cortex
Pla	plantar
TAO	total 'atypical' osteons

KARGER

Fax +41 61 306 12 34
E-Mail karger@karger.ch
www.karger.com

1422–6405/07/1854–0285$23.50/0

Accessible online at:
www.karger.com/cto

Dr. John G. Skedros
Utah Bone and Joint Center
5323 South Woodrow Street, Suite 202
Salt Lake City, UT 84107 (USA)
Tel. +1 801 713 0606, Fax +1 801 713 0609, E-Mail jskedros@utahboneandjoint.com

Introduction

Bone microdamage that occurs during normal activities [Burr et al., 1985; Vashishth et al., 2000; Skedros et al., 2003; Sobelman et al., 2004; Da Costa Gómez et al., 2005] has been implicated in skeletal fragility in elderly humans and in stress fractures in healthy young adults [Schaffler, 2001]. Experimental data suggest that *accommodating* microdamage formation in cortical bone may be more effective in curbing the incidence of fatigue failure than by purely *resisting* microdamage formation [Burr et al., 1988; Reilly et al., 1997; Martin et al., 1998; Reilly and Currey 1999, 2000; O'Brien et al., 2003]. In other words, allowing some microdamage to form (as long as it is not excessive) may be more efficient than morphologic adaptations that would be necessary to avoid the formation of microdamage altogether [Martin, 2003a, b]. The capacity of bone to accommodate/resist microdamage formation/propagation through microstructural/ultrastructural modifications is called 'toughening'.[1] One of the most important toughening mechanisms includes the introduction of microstructural *interfaces* such as cement lines of secondary osteons[2] [Ural and Vashishth, 2005; Gibson et al., 2006; Diab and Vashishth, 2007] (fig. 1, 2).

Recent studies demonstrate that osteons can express three-dimensional complexity that can significantly affect toughening by dissipating energy during microdamage propagation [Akkus et al., 2004; Nalla et al., 2005] (fig. 2, 3). This observation is important because it suggests that the synthetic capacities of osteoblast/osteoclast basic multicellular units (BMUs) are sufficiently plastic to enhance toughness by modifying osteonal morphology [Martin et al., 1996a; Hiller et al., 2003; Skedros et al., 2006b]. However, detecting this adaptation is difficult, especially since osteon distributions and morphologies are typically analyzed in two-dimensional images. Determining the mechanism(s) that mediate this plasticity poses a compelling challenge for understanding the various ways that osteons influence skeletal biomechanics.

In the present study we examined two-dimensional backscattered electron images in the perspective that they convey important information about how three-dimensional osteonal morphology correlates with regions where enhancements for toughening are expected. In this context, in addition to considering 'normal' osteon distributions, other osteonal characteristics, which we describe as 'atypical' (see fig. 4), were evaluated because they are considered potentially useful. It is unclear, however, if 'atypical' osteons are useful in this way, especially if many of these morphologic atypical 'types' are incidental consequences of osteonal branching (fig. 5) or natural variations resulting from the process of new osteon formation. For example, in a three-dimensional study of secondary osteon morphology, Stout et al. [1999] caution about using this nomenclature:

> Our results also suggest that some previously defined morphological 'types' of osteons may not exist, but rather are artifacts of the relative orientation of the plane of sectioning, or where along the length of a Haversian system the section was made. An example of this is the description of a dumbbell-shaped system in a discussion of the effects of geometry and collagen orientation

Fig. 1. Backscattered electron micrographs of cortical bone from the mid-diaphysis of a wild mule deer calcaneus. **A** Dorsal 'compression' cortex. **D** Plantar 'tension' cortex. The secondary osteons in the dorsal cortex are clearly smaller and more circularly shaped than those in the plantar cortex. These osteon size and the associated differences in secondary osteon population densities (highest density in the dorsal cortex) may reflect strain mode-related enhancements of osteon pullout resistance, which influences toughness and fatigue resistance. The plantar cortex, in addition to having obviously larger and more irregularly shaped osteons, also exhibits more active renewal – increased prevalence of newly forming osteons [i.e., darker osteons (lower mineralization, hence younger), newly forming osteons, and resorption spaces]. It is plausible that this active renewal accounts for the increased osteon heterogeneity in this region. Backscattered electron micrographs from the medial cortex (**B**) and lateral cortex (**C**) show increased prevalence of elongated osteons. We have hypothesized that increased prevalence of elongated osteonal variants are correlated with the prevalent/predominant shear in these neutral axis regions, and/or to their 'mixed' loading conditions (medial cortex = 'compression/shear'; lateral cortex = 'tension/shear') [Su et al., 1999; Sorenson et al., 2004; Skedros et al., 2006c].

[1] Toughness refers to the amount of energy required to fracture a material; the more the overall amount of energy consumed, the 'tougher' the material [Zioupos and Currey, 1998]. Tough materials resist damage propagation but do not necessarily resist damage formation. Toughness tests typically involve propagating a crack in a controlled direction through a specimen machined into a specific shape for this test. Toughness measurements obtained from these 'formal' toughness tests are different from the 'toughness' that is often 'informally' used to describe the energy absorbed by a specimen during a more conventional failure test. In this case, energy absorption is measured as the area under the stress/strain curve [Turner and Burr, 1993], which is an indirect measure of propagation toughness [Vashishth, 2004].

[2] Secondary osteons (Haversian systems), which result from BMU activity and define secondary bone, form quasi-cylindrical cores (~140–200 μm diameter) of solid lamellar bone with multiple cylindrical/concentric lamellae that surround a central canal for blood vessels. An additional feature that distinguishes secondary osteons from primary osteons (i.e., primary vascular canals) is the well-defined peripheral boundary (cement line) between the osteon and the surrounding tissue [Currey, 2002].

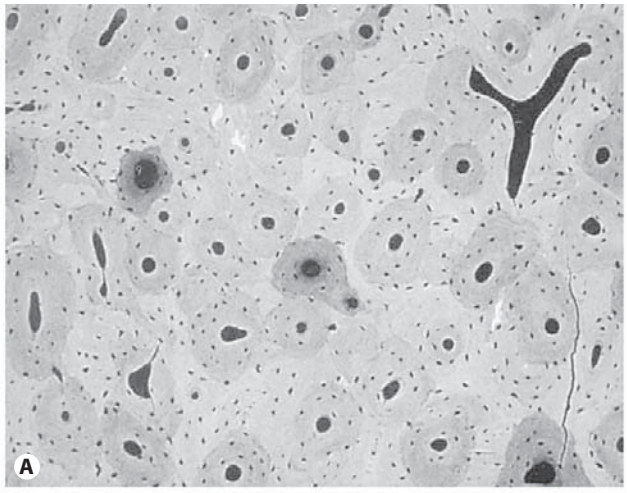

Dorsal 'Compression'

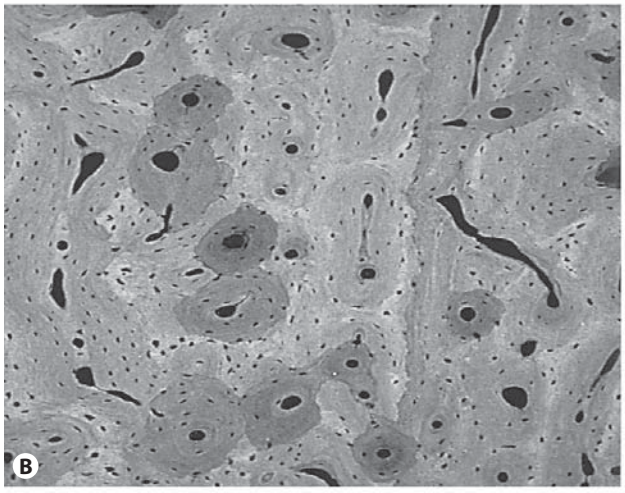

Medial

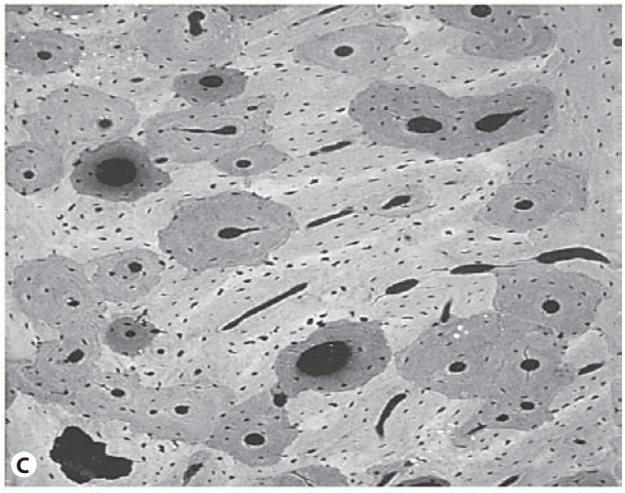

Lateral

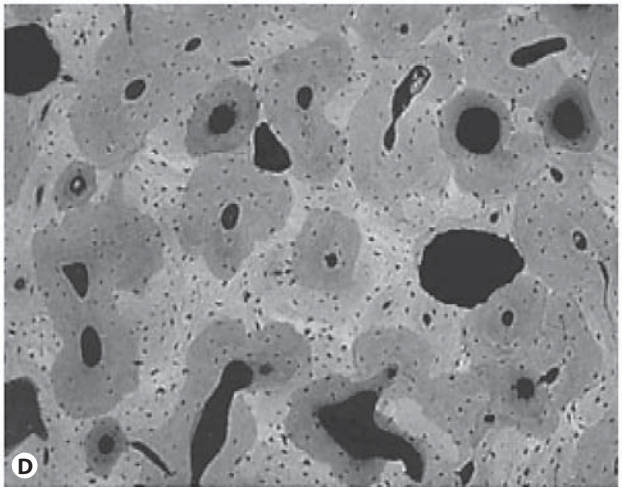

Plantar 'Tension'

100 µm

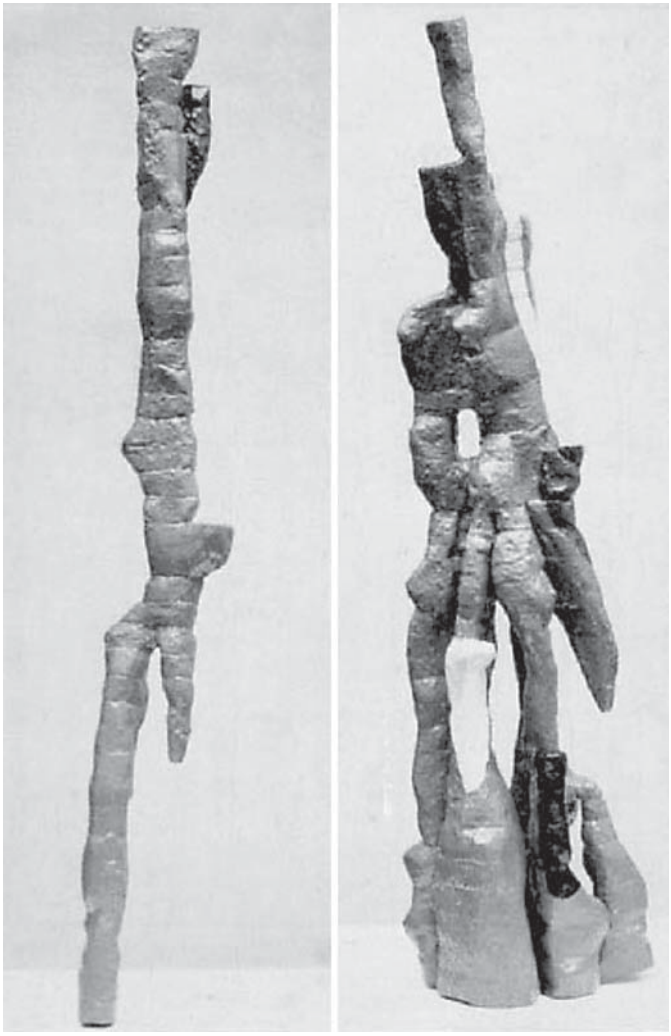

Fig. 2. Photographs of three-dimensional reconstructions of secondary osteons from mid-third diaphyses of a dog femur. They demonstrate the three-dimensional complexities of branching of 'single' osteons as they course through the bone [reproduced with permission from Cohen and Harris, 1958, with permission of the publisher, American Academy of Orthopaedic Surgeons] (see also [Mohsin et al., 2002]).

on the biomechanical properties of osteons [Pidaparti and Burr, 1992]. We have determined that this dumbbell-shaped system is produced by sectioning through an osteon branch.

In this context, the 'atypical' morphological variants E-I in figure 4 are most likely manifestations of the degree of osteonal interconnections, and, therefore, we avoid describing them as osteon 'types'.

In some loading environments, however, some 'atypical' osteons may be 'typical', reflecting possible mechanically important microstructural complexities such as those shown in figure 1. For example, osteons that have been shown to course obliquely to a bone's long axis possibly reflect adaptations for prevalent/predominant shear produced by habitual torsion – such as in diaphyses of sheep tibiae [Lanyon and Bourn, 1979] and radii [Mohsin et al., 2002], and canine and human femora [Cohen and Harris, 1958; Petrtýl et al., 1996]. Obliquely coursing osteons would be seen in transverse section as elongated osteons (variant D in fig. 4). There are many additional examples showing how secondary osteons can course obliquely, become extensively interconnected, and/or exhibit directional changes, including studies of drifting osteons [Robling and Stout, 1999] and osteons in shear/torsion environments [Stover et al., 1992; Skedros et al., 1997; Sorenson et al., 2004] or in complex mechanical environments near implanted devices such as metal screws and tooth fixtures [Albrektsson and Johansson, 1991]. Studies of the microstructural organization of deer calcanei also suggest that the significant differences between the dorsal, plantar, and medial/lateral cortices in the prevalence of osteonal variants [Skedros et al., 1994b; Sorenson et al., 2004] may represent differential adaptations that toughen regions by minimizing microdamage formation and/or propagation in their respective habitual strain modes (i.e., tension, compression, or shear) [Anderson and Skedros, 2005] (fig. 1, 3). Such microstructural adaptations that accommodate tension, compression, or shear strain[3] are expected since mechanical properties of cortical bone (including fatigue behavior and microdamage mechanics) significantly differ in these strain modes [Burstein et al., 1976; Carter and Hayes 1977b; Boyce et al., 1998; Reilly and Currey, 1999]. Mechanical testing data support the hypothesis that the regional prevalence of osteonal variants in deer calcanei are significantly correlated with energy absorption (toughness) [Vajda, 1998].

The morphology (e.g., size, shape, and length), direction of propagation, and incidence of matrix microdamage in fatigue-loaded bone is also highly dependent upon

[3] Mechanical strain is the change in length of a loaded structure as a percentage of its initial (unloaded) length. (Note: Shear strain is not a change in length but a change in angle.) This dimensionless ratio is a measure of material or tissue deformation. In vivo strain data from a variety of animals suggest that physiologically strains are generally between 200 and 3,000 microstrain (i.e., between 0.02 and 0.30% change in length) in compression [Biewener et al., 1983a, b; Rubin and Lanyon, 1985]. The upper limit may be only 1,500 microstrain in tension [Fritton et al., 2000]. For an isotropic material loaded axially, stress and strain are related by Hooke's law, which says that they are proportional to one another. Available data suggest that strain is the mechanical parameter most directly involved in causally mediating bone adaptations [Rubin and Lanyon, 1984; Lanyon, 1987; Ehrlich and Lanyon, 2002].

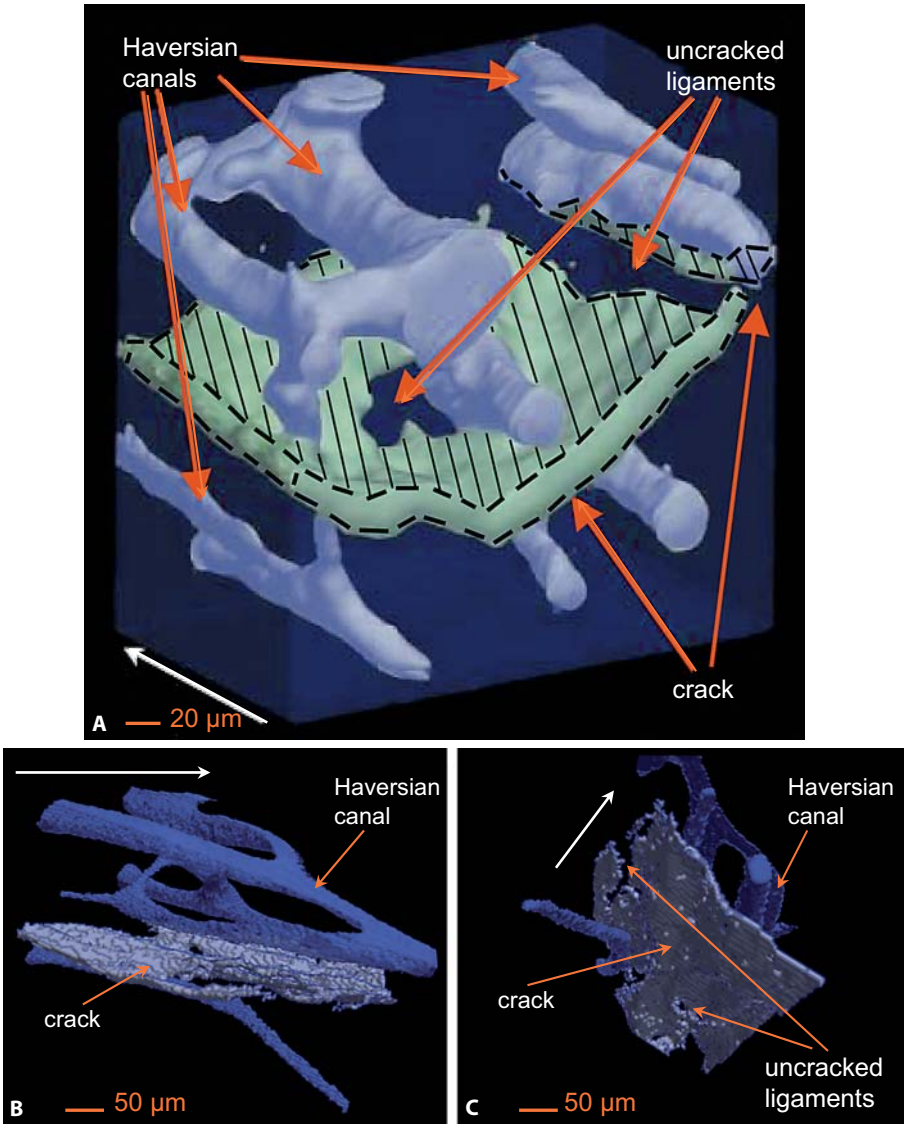

Fig. 3. Three-dimensional microtomographic reconstructions showing microcracks traveling along, and being diverted by, cement line regions of secondary osteons exhibiting three-dimensional complexity (branching, obliquity, and interconnections). Note that the central canals of the osteons are shown; however, the microcracks are actually located at the peripheries of the osteonal walls (i.e., near the cement lines; R.O. Ritchie, pers. commun.). **A** The microcrack resembles a 'canopy' (the cross-hatched lines indicate the area of the crack and its margins are indicated with dashed lines) that appears to follow the cement lines bordering the osteons. **B**, **C** Similarly, microcracks can be seen that have propagated along cement lines. In this figure, uncracked segments are denoted as uncracked 'ligaments' [reproduced with slight modification from Nalla et al., 2005 with permission of the publisher, Elsevier Science, New York, N.Y.].

strain mode [Carter and Hayes, 1977a; Boyce et al., 1998; Reilly and Currey, 1999; Akkus et al., 2003; George and Vashishth, 2005]. This is important when interpreting putative mechanical relevance(s) of varying degrees of osteonal remodeling, and regional variations in the prevalence of osteonal variants, because in vivo strain measurements from bones of various mammalian and avian species during peak loading of controlled ambulation typically demonstrate directionally consistent bending (producing a habitual tension/compression/shear strain distribution) or torsion (producing habitual shear) [Lanyon and Baggott, 1976; Lanyon et al., 1979; Rubin and Lanyon, 1985; Biewener et al., 1986; Swartz et al., 1992; Szivek et al., 1992; Biewener and Bertram, 1993; Biewener and Dial, 1995; Demes et al., 1998; Coleman et al., 2002; Lieberman et al., 2004]. In turn, a consistent tension/compression/shear strain distribution might be correlated with regional differences in microdamage morphology that reflect differences in osteonal morphology as a result of the repair process. However, it is not known if mechanical/toughening implications for the prevalence and/or distribution of 'typical' or 'atypical' osteons are generally applicable among mammalian bones exhibiting secondary osteon formation. For example, in some cases, the prevalence of some regional osteonal morphologic variants could simply be the product of increased remodeling activity and/or metabolic activity (e.g., osteon variants in fig. 4A–C) such as is thought to occur near

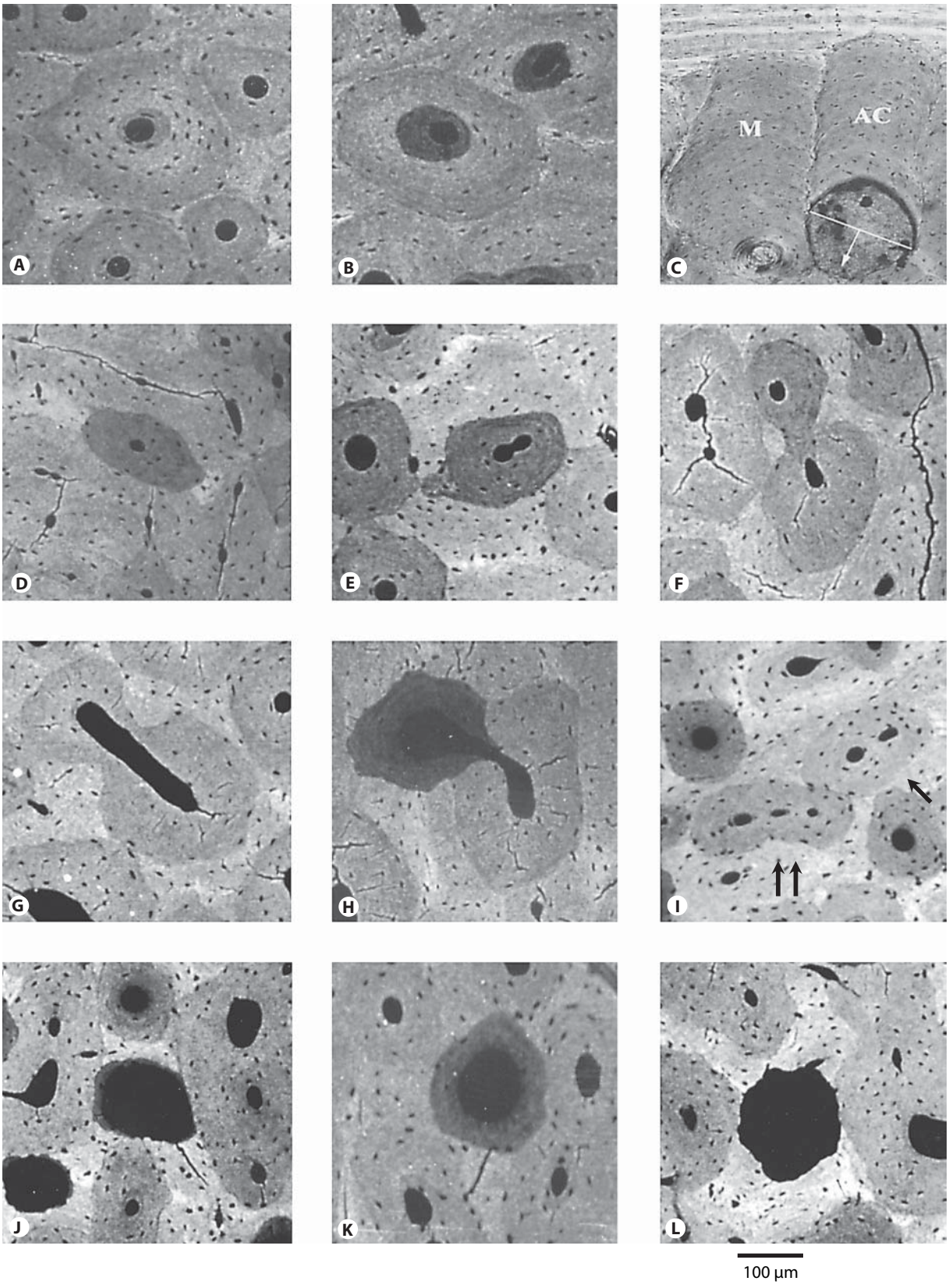
A
B
C
M
AC
D
E
F
G
H
I
J
K
L
100 µm

marrow cavities and in low strain regions (e.g., endosteal cortical regions) [Weidmann, 1956; Nelson et al., 1960; Knese and Titschak, 1962; Skedros et al., 1997; Bousson et al., 2001; Rauch et al., 2007].

The most comprehensive studies on spatial distributions of osteonal variants that we could locate are those of Knese and coworkers [Knese et al., 1954a, b; Knese and Titschak, 1962; Knese, 1979]. They described the distribution and quantity of different forms of osteons within the same cross section of long bones from upper and lower extremities of modern human adults [Knese et al., 1954b] and principal metacarpals (MC3, MC4) of pigs (6 months to 4 years) and wild boars (8 months to 7 years) [Knese and Titschak, 1962]. Although these investigators thoroughly describe transcortical variations in the prevalence of osteonal variants, with up to 15 different osteon 'types' described, they did not attempt to determine if they correlated with habitual strain mode or magnitude. The main goal of the present study (specific hypotheses are below) is to examine patterns in the spatial distributions of osteonal variants such as those in figure 4 as potential adaptations. This was accomplished by examining their spatial distributions for correlations with strain distributions and other material characteristics (e.g., secondary osteon population density, new remodeling events, and predominant collagen fiber orientation) in bones with well-known loading histories. These data are also presented in the perspective of a literature review (see Appendix) of studies describing how two-dimensional osteon data might be useful for interpreting local load history or metabolism.

Fig. 4. Secondary osteon variants and related characteristics. **A** Double zoned: Secondary osteons that exhibit a hypercalcified ring within the lamellae of the osteon. This ring is thought to reflect a slowing or temporary cessation of infilling during osteon formation. Pankovich et al. [1974] defined double-zoned osteons as 'a system that exhibited either an abrupt change in mineral density or one or more growth arrest lines' (see Appendix). In the present study, in most cases it was not possible to confidently distinguish double-zoned from embedded osteons (see below). **B** Embedded (or 'double zoned'): Smaller versions of common secondary osteons that form within, but do not cross, the cement line of a preexisting secondary osteon (see 'double-zoned' description). **C** Mature (M) drifting: Secondary osteons exhibiting a noncentrally located central canal surrounded by 4–8 concentric lamellae, which on one side are continuous with a hemicyclic deposited 'tail' of lamellae. Actively (AC) drifting: a secondary osteon that exhibits a history of continuous resorption on one side and continuous formation on the other; as a result the osteon becomes flattened in one plane and elongated transversely to this plane. The arrow indicates direction of drift of the osteon on the right [reproduced from Robling and Stout, 1999, with permission of the publisher, S. Karger AG, Basel, Switzerland]. **D** Elongated: A secondary osteon in which the length of one axis (or diameter) is at least 2 times the length of the short axis (or diameter). By definition, an elongated osteon cannot be a dumbbell osteon (see below). **E** Connected singlet: A secondary osteon containing two or more central canals within a single cement line boundary, and these canals are confluent. **F** Dumbbell: A secondary osteon where two or more *nonconfluent* central canals are contained within a single cement line boundary and there is 30% or greater constriction between the canals (i.e., the osteon is narrowed by ≥30% of its diameter). **G** Dumbbell connected: A dumbbell secondary osteon with two or more confluent canals within a single cement line boundary. **H** Connected doublet: Two secondary osteons that partially overlap but do not exhibit dumbbell-like constriction (see above), and have confluent canals. **I** Multiple canals: A secondary osteon with two or more *nonconfluent* canals contained within a single cement line boundary. These osteons are indicated with arrows (the two arrows indicate a multiple canal osteon that is also elongated). **J**, **K** Newly forming osteons: Secondary osteons with relatively poorly mineralized bone, seen as relatively darker gray levels in the backscattered electron images, and less than one half of complete radial closure. **L** Resorption space: A porous space characterized by scalloped edges and the absence of observable mineralized bone in backscattered electron images or microradiographs. Cross-sectional areas of resorption spaces are also within the range of secondary osteon cross-sectional areas.

Specimens, Habitual Strain Environments, and Hypotheses

All of the bones examined (radii, MC3, and calcanei of horses, and calcanei of sheep, deer and elk) are characterized by torsion and/or habitual bending, the latter producing a neutral axis with a consistent location during peak loading of typical gaits. Although a comparatively large shift in the neutral axis can occur (indicative of torsion, fig. 6) in the equine MC3 as gait speed increases [Gross et al., 1992; Nunamaker, 2001], the neutral axis of many long bones of the limb is generally in a consistent location during peak loading. Cortices along a habitual neutral axis generally undergo normal strains[4] that are oblique to the long axis of the bone, and shear strains that are generally more prevalent/predominant (i.e., where shear strains are not generally dominated by longitudinal tension or compression) [Drucker, 1967]. While shear

[4] In past studies we have often referred to these as principal strains. However, this usage is inexact because principal strains are the orthogonal strains in the directions in which shear strain becomes zero [Gere and Timoshenko, 1984].

Fig. 5. Outline drawings of osteons from a serially sectioned plantar 'tension' cortex of a deer calcaneus. These images (**A–F**) show how osteon morphology, interconnections, and interdigitations can change within only a few hundred microns of osteon length; it is suggested that this three-dimensional interfacial complexity serves to enhance toughness (see fig. 3). The tissue was demineralized and paraffin embedded, and sectioned at 20 µm with a microtome blade (there is no kerf loss). As indicated, the drawings were made from sections either 80 or 40 µm apart. The curved line at the lower left of each drawing is the margin of a longitudinally oriented (i.e. orthogonal to the plane of the transverse section) drill hole made in the central portion of the cortex. Changes in the relative placement of the osteons away from the margin of the drill hole (suggesting three-dimensional changes in orientation) are accurate; i.e., they are not artifacts of field selection. The following changes are notable: (1) osteon No. 1 splits into two osteons and has embedded osteons (dashed lines) within it, (2) osteon No. 2 forms an osteon 'conglomerate' (**D–F**, upper left), (3) two osteons labeled No. 3 and No. 4 in **A** merge to form a multicanal osteon that divides again (**D**) and merges into an osteon 'conglomerate' (the question marks indicate that it becomes difficult to identify osteons 2, 3 and 4 in the conglomerate), and (4) osteon No. 5 has an embedded osteon associated with it (**D**, **E**) and then becomes a multiple-canal osteon (**F**).

strains exist throughout the bone cross section, this is the prevalent strain mode along the neutral axis, since bending loads, superimposed on torsional and axial loading, would eclipse the shear strains in the habitual tension and compression regions. Because of eccentric external loading of each bone type (i.e., predominant loading oblique to the long axis of each bone), the 'compression' cortices also experience the highest strains [Lieberman et al., 2004]. Each cortical location (e.g., dorsal, plantar, medial, and lateral) also typically experiences highest strain on the periosteal surface, and lowest strain on the endosteal surface.

Hypotheses

The spatial distributions of the osteon variants (fig. 4) were evaluated in the context of the hypotheses listed be-

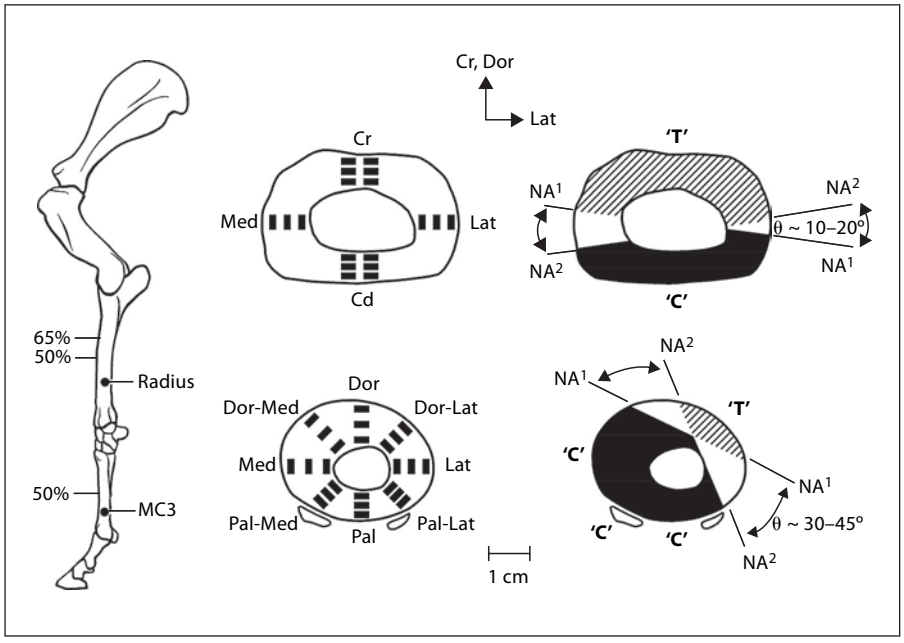

Fig. 6. Lateral-to-medial view of a left forelimb skeleton of an adult horse showing the radius and MC3. At near right are cross sections showing image locations, and at far right are the approximate typical ranges subtended by the neutral axes (NA) during weight bearing. Several studies reporting in vivo strain data were used to create these drawings [Turner et al., 1975; Rubin and Lanyon, 1982; Schneider et al., 1982; Biewener et al., 1983a, b; Gross et al., 1992]. Changes in neutral axis locations for the equine MC3 are considered in table 1 as two 'tension' regions and four 'compression' regions. 'C' = Compression region (darkened); 'T' = tension region (oblique lines); Cr = cranial; Cd = caudal; Dor = dorsal; Pal = palmar; Med = medial; Lat = lateral.

low. While these osteonal variants are clearly related to the remodeling process, they can be segregated into different subgroups that might have varying implications for mechanical properties. For example, osteons that produce increased cement line interfaces when compared to other osteon variants, and that could, in turn, enhance toughness for a prevalent/predominant strain mode, are grouped as 'category DED' osteons (drifting, elongate group, and doublet-connected osteons; fig. 4C, D, H). The genesis of hypotheses 1 and 2 is based on the idea that these osteons would be more prevalent in regions where the putative requirement of osteonal interfacial complexity would be most obvious. We also consider the possibility that increased prevalence of zoned and embedded osteons, and newly forming osteons, if mechanically relevant, may enhance local 'toughening' by their association with variations in porosity and mineralization (see Appendix). An osteon heterogeneity index (OHI) is also used as a means for estimating the extent that an osteon characteristic or category is related to the local population densities of all secondary osteons. The hypotheses examined are:

(1) Increased prevalence of osteons that have high interfacial complexity (i.e., DED group) will occur in 'shear' and 'tension' cortices as opposed to 'compression' cortices, as a possible means for differentially enhancing toughness by adjusting osteonal cement line complexity (e.g., orientation and interconnections).

(2) Equine MC3s will generally have more prevalent osteons that increase interfacial complexity (i.e., DED group) compared to each of the other bones examined in this study, since habitual torsional loading may produce more uniformly distributed shear stresses. Stronger support for this hypothesis might also include data showing more prevalent elongated osteons in MC3s when compared to the other relatively more simply loaded bones (equine radii, and calcanei of sheep, deer, elk, and horses).

(3) Since remodeling activity is generally thought to be greater in endosteal regions than in periosteal regions, increased prevalence of osteonal variants (any of the variants) will be found near the medullary canal (i.e., endosteal regions) than near the periosteum.

Correlation analyses were also conducted in order to detect possible relationships of the various osteonal variants with additional structural and material characteristics of these bones.

Materials and Methods

Equine Radii and MC3s (fig. 6)

Ten radii and nine MC3s were obtained from skeletally mature standard-breed and quarter horses with no history of racing or race training and no evidence of skeletal pathology at the time of death. Only one bone was obtained from each animal. The bones had been used in previous studies reporting correlations of vari-

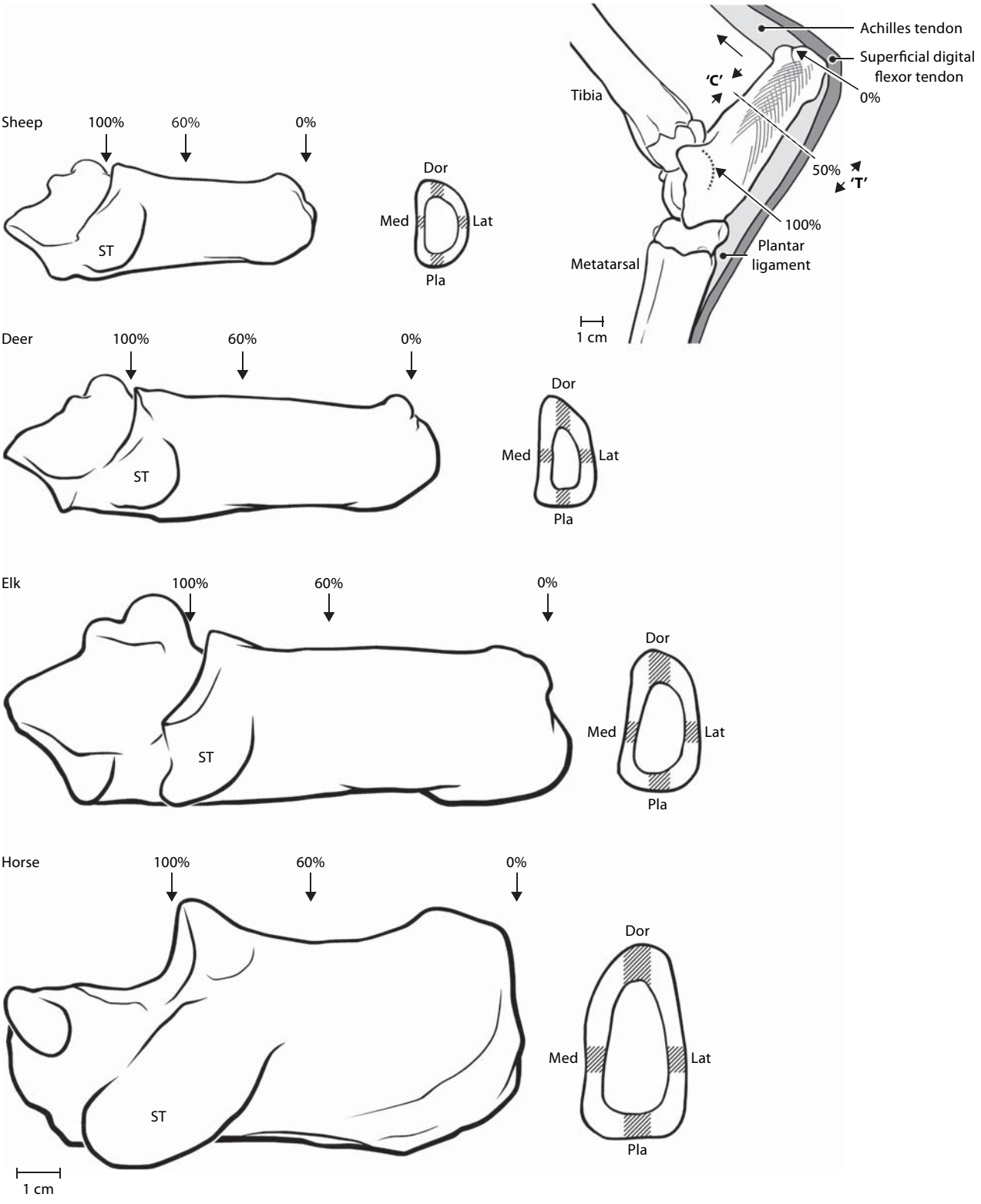
Sheep
100%
60%
0%
ST
Dor
Med
Lat
Pla
Deer
100%
60%
0%
ST
Dor
Med
Lat
Pla
Elk
100%
60%
0%
ST
Dor
Med
Lat
Pla
Horse
100%
60%
0%
ST
Dor
Med
Lat
Pla
1 cm
Achilles tendon
Superficial digital flexor tendon
'C'
0%
Tibia
50%
'T'
100%
Plantar ligament
Metatarsal
1 cm

ous material characteristics with habitual strain environments from the mid-third of the bone (radius) or at mid-diaphysis (MC3) [Mason et al., 1995; Skedros et al., 1996, 2005]. Each bone had been manually cleaned of soft tissue and sectioned transversely at 50% of its length (MC3), or at 50 and 65% of its length (radius). One 5-mm-thick segment was cut from each bone immediately distal to these transection levels. The undecalcified, unstained segments were embedded in polymethyl methacrylate using conventional techniques [Emmanual et al., 1987] and subsequently ground, polished and prepared for backscattered electron imaging [Skedros et al., 1993].

In the MC3s, two to three 50× high-resolution backscattered electron micrographs (1.6 × 2.3 mm) were taken within each of the three transcortical 'envelopes' or regions [i.e., periosteal ('outer'), middle cortical, endosteal cortex ('inner')] in octant locations: dorsal (Dor), dorsal-lateral (Dor-Lat), lateral (Lat), palmar-lateral (Pal-Lat), palmar (Pal), palmar-medial (Pal-Med), medial (Med), and dorsal-medial (Dor-Med) for a total of 24 image locations (fig. 6). In the radii, two 50× (2.71 × 2.71 mm) backscattered electron micrographs were taken within each of the three regions of the cranial (Cr) and caudal (Cd) cortices, and one image in each region of the medial and lateral cortices for a total of 12 image locations in each section.

Calcanei of Horses, Elk, Sheep and Deer (fig. 7)

One calcaneus was obtained from each of seven standard-breed horses with no history of racing or race training, seven wild-shot North American elk *(Cervus elaphus)*, and seven domesticated sheep *(Ovis aries)*. All of these bones were from adult animals that had been used in previous studies [Skedros et al., 1997]. All elk were males, had shed the periosteal cover of their antlers, and were obtained from their natural habitat in a fall hunting season. The horse calcanei were from mixed sexes that had been set to pasture, and were not from the same animals from which the radii and MC3s were obtained. The horses were between 2 and 9 years old. The sheep were females and approximately 2 years old. The sheep and horses had been kept in large pastures. Calcanei were also obtained from 10 wild-shot skeletally mature male deer used in previous studies [Skedros et al., 1994a, b; Skedros, 2005].

Transverse segments, 4–5 mm thick, were cut from the sheep, elk, and horse calcanei at 60% of shaft length. The deer calcanei were sectioned at both the 50 and 70% locations. These unstained, undecalcified segments were embedded in polymethyl methacrylate using conventional methods [Emmanual et al., 1987]. The proximal face of each segment was ground, polished and prepared for backscattered electron imaging utilizing the same techniques employed for the equine radii and MC3s. One 50× backscattered electron image representing 3.41 mm^2 (2.23 × 1.53 mm) was obtained in each transcortical region (periosteal, middle cortical, endosteal) of the dorsal 'compression' and plantar 'tension/shear' cortices of each specimen. (Because of narrow caudal cortices of the sheep calcanei, only two images were obtained, but the area imaged was analyzed in three intracortical regions of equal area.) The images excluded circumferential lamellar bone. One image was also taken within each medial and lateral cortex.

Fig. 7. All calcanei in medial-to-lateral view; from top to bottom: sheep, deer, elk, and horse. Cross sections show image locations in 'gray'. One section (60% location) was analyzed in sheep, elk, and horse bones, and two sections (50 and 70% locations) were analyzed in deer bones. Dor = Dorsal, Pla = plantar, Med = medial, Lat = lateral. The inset drawing at the upper right shows an adult right deer calcaneus in lateral-to-medial view showing typical loading along the Achilles tendon (large arrow) producing net compression ('C') and tension ('T') on dorsal and plantar cortices, respectively. This loading regime is similar in all of the calcanei. ST = Sustentaculum talus.

Histomorphometric Analyses

Complete secondary osteons were identified and manually counted in the images. Conventional point counting techniques were used for determining porosity and the fractional area of secondary osteonal bone (On.Ar/T.Ar) [Skedros et al., 1997]. The fractional area of secondary osteonal bone was defined as the total area of secondary bone (S) divided by the total area of secondary bone plus interstitial bone (I): [S/(S + I)]. Newly forming secondary osteons were identified using two criteria: (1) the presence of relatively recently mineralized bone (seen as darker gray levels in the backscattered electron images) and (2) incomplete radial closure (i.e., incomplete centripetal deposition) of the recently mineralized bone. To determine if the second criterion was satisfied, two mutually orthogonal lines (cranial-caudal and medial-lateral directions) were drawn on each apparent newly forming osteon. Incomplete radial closure was defined as mineralized bone extending less than one half of two or more of the four radii.

For collagen fiber orientation analyses, segments of the bone embedded in polymethyl methacrylate were ultra-milled to 100 ± 5 μm and analyzed using circularly polarized light. Regional differences in predominant collagen fiber orientation were quantified in terms of corresponding differences in the transmitted light intensity, where darker gray levels (lower numerical values) represent relatively more longitudinal collagen and brighter gray levels (higher numerical values) represent relatively more oblique-to-transverse collagen. The methods that were used to quantify regional collagen fiber orientation differences in cortical bone as differences in gray levels [Boyde and Riggs, 1990; Skedros et al., 1996] have produced relative differences that are similar to the 'longitudinal structure index' described by Martin and coworkers [Martin and Burr 1989; Martin et al., 1996b] and used recently [Takano et al., 1999; Kalmey and Lovejoy, 2002].

Quantification of Osteon Variants

Atypical secondary osteons (osteon variants) were determined using criteria described in figure 4. The osteon variants and new remodeling events (=resorption spaces and newly forming secondary osteons) were manually counted by two trained assistants. The images were also randomly assorted and evaluated by the two blinded observers. After independent reevaluation of a subgroup of images by the principal investigator it was determined that both intraobserver and interobserver error was ~1.5%.

The prevalence of these osteonal variants was also examined in the context of the degree of remodeling, which was quantified with respect to regional population densities of new remodeling events. Since the tissues that we used were not fluorochrome labeled, and osteoid is not detectable in backscattered electron images, the criteria used for distinguishing new remodeling events from more mature secondary osteons included the presence of

(1) relatively poorly mineralized bone, seen as darker gray levels in backscattered electron images and (2) less than one half of their radial closure [Skedros et al., 1997]. New remodeling events were quantified since their prevalence can reflect the degree of active renewal, such as occurs during growth, exercise of sufficient duration or intensity, some diseases (e.g., high-turnover osteoporosis), and conditions of low strain [Martin and Burr, 1989; Skedros et al., 1997; Martin et al., 1998; Lieberman et al., 2003; Skedros and Hunt, 2004]. This analysis helps to determine if spatial variations in the prevalence of osteon variants are associated with the degree of active remodeling (i.e., where their formation becomes statistically more likely with increased remodeling activity). Additional analyses were also conducted to determine if regional variations in the prevalence of osteon variants are correlated with the amount of remodeled bone (i.e., percent secondary bone), local cortical thickness, and, for some bones, predominant collagen fiber orientation (see below).

The osteon variants were evaluated separately and in subgroups. The subgroups included: (1) zoned group (fig. 4A, B), (2) connected group (connected elongate, fig. 4E, G, H), (3) drifting group (fig. 4C), (4) elongated group (connected and multicanal elongate, fig. 4D, F, G), (5) multicanal group (connected and multicanal elongate, fig. 4D, E, F, G), and (6) DED group (fig. 4C, D, H), or osteons that increase interfacial complexity when compared to the other osteon variants. The population densities of total 'atypical' osteons were also quantified in each cortical location. Using this value, an 'osteon heterogeneity index' ($OHI_{(A)}$) was calculated: [(total 'atypical' osteons)/(number of all complete secondary osteons/mm^2 bone)] (this includes lacunar and central canal porosity, but excludes other porosities). Secondary osteons in each image had been determined in previous studies [Skedros et al., 1994a, b; Mason et al., 1995; Skedros et al., 1997]. A second OHI included only the osteons that would clearly increase cement line interfaces – the DED group (i.e., $OHI_{(DED)}$).

Statistical Analyses

A three-way ANOVA design was used to analyze data from equine radii [section location, cortex (quadrant), intracortical 'region'], and a two-way ANOVA was used for data from equine MC3s (cortex, intracortical 'region') and deer calcanei (section location, cortex). In most analyses of the MC3s, only quadrant [dorsal (Dor), palmar (Pal), medial (Med), and lateral (Lat)] data were used. Octant data for MC3s were used for 'strain mode area' comparisons. A one-way ANOVA was used for data from the sheep, elk, and horse calcanei. Analyses in the calcanei did not consider intracortical 'region' as a factor, since in their medial and lateral cortices no distinction was made for periosteal (Pe), middle (Mi), and endosteal (En) 'regions'. All possible pairwise comparisons between quadrant locations and transcortical 'regions' within each quadrant were assessed for statistical significance ($\alpha \leq 0.05$) using the nonparametric Kruskal-Wallis Z post-hoc test [J. Hintze, NCSS Version 6.0, Kaysville, Utah; http://www.ncss.com; Gibbons, 1976]. Since the data are nonparametric and the relatively large number of comparisons could increase type 1 errors, an alpha level of ≤ 0.01 was used for statistical significance in the two- and three-way ANOVAs.

Strain mode (tension, compression, and shear) comparisons were also conducted for each bone. In the calcanei the 'compression' area was considered to be the dorsal cortex, the 'tension/shear' area the plantar cortex, and the 'neutral axis' ('shear regions') the medial and lateral cortices (fig. 7). In the equine radii, the 'compression' area was considered the caudal cortex, the 'tension' area the cranial cortex, and the 'neutral axis' the medial and lateral cortices (fig. 6). The 'tension' and 'compression' areas (cortical 'locations') of the MC3s that were based on octants are shown in table 1.

Correlation Analyses

The additional structural and material characteristics used in the correlation analyses have been reported in previous studies [Skedros et al., 1994a; Mason et al., 1995; Skedros et al., 1996, 1997, 2004] and include: (1) secondary osteon population density (number of osteons/mm^2 bone), (2) fractional area of secondary bone expressed as a percentage [(number of osteons/mm^2 bone)·100], (3) population density of new remodeling events, (4) predominant collagen fiber orientation expressed as a weighted mean gray level in circularly polarized images from subsets of only the deer calcanei, and equine radii and MC3s, and (5) cortical thickness of quadrant cortical locations in all bones.

Results

Results are summarized in tables 1–4 and figures 8 and 9. Results of two- and three-way ANOVAs in the deer calcanei (section location, cortex), equine MC3s (cortex, intracortical 'region'), and equine radii (section location, cortex, intracortical 'region') did not show significant differences or interactive effects between these factors in each species (table 3).

Hypothesis 1 states that 'atypical' osteons that increase interfacial complexity (i.e., DED group) would be more prevalent in cortices experiencing predominant/prevalent tension or shear, perhaps representing adaptations for the specific mechanical properties required in these strain environments. With some exceptions, analysis of DED osteons and the 'osteon heterogeneity index' with respect to the DED group [$OHI_{(DED)}$] in quadrant comparisons in *all* bones did not support this hypothesis (table 3). Exceptions include the equine MC3s, which showed significantly higher DED osteons and $OHI_{(DED)}$ in the dorsal 'tension' cortex than in the palmar 'compression' cortex ($p < 0.05$), and the deer calcaneus, which had significantly higher DED osteons and $OHI_{(DED)}$ in the plantar 'tension' cortex than the dorsal 'compression' cortex ($p < 0.05$). The equine radii also exhibited significantly higher $OHI_{(DED)}$ in the cranial 'tension' cortex than in the caudal 'compression' cortex ($p < 0.05$). The lateral cortex of the MC3s also showed significantly higher DED osteons and $OHI_{(DED)}$ than the dorsal 'compression' cortex ($p < 0.05$). While these exceptions might be important findings that tend to support hypothesis 1 for a specific species, the lack of consistent findings among *all* the spe-

Table 1. Structural and material characteristics by strain mode areas

Cortical locations	Total atypicals, n/mm^2	OHI$_{(A)}$	DED group n/mm^2	On.N/T.Ar n/mm^2	On.Ar/T.Ar %	Porosity %	CFO WMGL
MC3							
Tension '1' (Dor, Dor-Lat, Lat)	1.31 (0.90)	0.10 (0.07)	0.47 (0.40)	14.4 (6.50)	36.0 (16.9)	4.70 (1.60)	129.1 (20.2)
Tension '2' (Dor-Lat, Lat)	1.33 (0.90)	0.07 (0.05)	0.47 (0.39)	13.7 (6.10)	35.3 (16.5)	4.50 (1.20)	119.6 (17.4)
'C1' (Pal-Lat, Pal, Pal-Med, Med, Pal-Med)	1.15 (0.83)	0.07 (0.05)	0.29 (0.30)	16.0 (7.40)	42.7 (16.4)	5.20 (2.10)	150.1 (30.0)
'C2' (Pal-Lat, Pal, Pal-Med, Med)	1.08 (0.72)	0.10 (0.07)	0.25 (0.30)	16.4 (7.10)	43.9 (15.5)	5.40 (2.30)	153.7 (28.6)
'C3' (Pal-Lat, Pal, Pal-Med)	1.13 (0.78)	0.07 (0.04)	0.27 (0.31)	16.6 (6.60)	44.4 (14.2)	5.60 (2.60)	158.5 (26.2)
'C4' (Pal, Pal-Med, Med)	1.07 (0.87)	0.07 (0.05)	0.28 (0.30)	16.1 (7.20)	43.1 (15.8)	5.40 (2.40)	156.8 (29.7)
Radius							
Cranial 'tension'	1.20 (0.70)	0.05 (0.00)	0.32 (0.32)	9.40 (5.20)	26.8 (15.2)	4.40 (2.00)	89.5 (24.6)
Caudal 'compression'	2.10 (0.99)	0.12 (0.08)	0.32 (0.35)	18.1 (4.50)	53.7 (12.0)	4.90 (1.70)	134.3 (32.7)
Medial	0.77 (0.60)	0.10 (0.10)	0.23 (0.30)	8.50 (4.90)	26.5 (17.4)	5.20 (1.70)	82.4 (22.9)
Lateral	0.81 (0.67)	0.12 (0.15)	0.22 (0.30)	8.30 (4.10)	24.9 (13.8)	4.90 (2.50)	83.6 (29.8)

Equine MC3 and radius tension ('T') vs. compression ('C') area comparisons. OHI = Osteon heterogeneity index [(total atypicals)/(On.N/T.Ar)]; On.N/T.Ar = number of secondary osteons/mm^2 of bone; On.Ar/T.Ar = fractional area of secondary osteonal bone expressed as %; C = compression; Dor = dorsal; Pal = palmar; Med = medial; Lat = lateral; Dor-Lat = dorsal-lateral; Dor-Med = dorsal-medial; Pal-Lat = palmar-lateral; Pal-Med = palmar-medial; CFO = predominant collagen fiber orientation expressed as a weighted mean gray level (WMGL).

Table 2. Calcanei: atypical osteon characteristics (n/mm^2; means and SD)

	Connected group	Drifting group	Elongate group	MC group	Zoned group	DED group	OHI$_{(DED)}$	Total atypicals	OHI$_{(A)}$	N.On/T.Ar
Horse										
Dor	0.05 ± 0.11	0.00 ± 0.00	0.18 ± 0.34	0.87 ± 0.64	0.09 ± 0.15	0.02 ± 0.07	0.00 ± 0.01	0.81 ± 0.66	0.04 ± 0.03	25.21 ± 7.66
Pla	0.00 ± 0.00	0.00 ± 0.00	0.18 ± 0.24	0.29 ± 0.32	0.22 ± 0.67	0.04 ± 0.09	0.00 ± 0.00	0.41 ± 0.65	0.02 ± 0.03	16.37 ± 5.57
Med	0.00 ± 0.00	0.00 ± 0.00	0.07 ± 0.20	0.52 ± 0.50	0.15 ± 0.40	0.00 ± 0.00	0.00 ± 0.00	0.60 ± 0.45	0.04 ± 0.04	16.51 ± 5.94
Lat	0.00 ± 0.00	0.00 ± 0.00	0.26 ± 0.21	0.90 ± 0.33	0.19 ± 0.29	0.00 ± 0.00	0.00 ± 0.01	0.82 ± 0.51	0.04 ± 0.03	20.17 ± 3.83
Elk										
Dor	0.07 ± 0.17	0.03 ± 0.10	0.14 ± 0.21	1.19 ± 0.61	0.14 ± 0.35	0.18 ± 0.21	0.01 ± 0.01	1.38 ± 0.66	0.06 ± 0.03	19.03 ± 5.27
Pla	0.01 ± 0.06	0.00 ± 0.00	0.21 ± 0.39	0.68 ± 0.63	0.00 ± 0.00	0.21 ± 0.40	0.01 ± 0.01	0.68 ± 0.63	0.03 ± 0.02	24.02 ± 6.64
Med	0.04 ± 0.10	0.00 ± 0.00	0.19 ± 0.25	1.09 ± 0.79	0.00 ± 0.00	0.18 ± 0.25	0.01 ± 0.01	1.12 ± 0.81	0.05 ± 0.03	22.7 ± 3.70
Lat	0.04 ± 0.10	0.00 ± 0.00	0.19 ± 0.25	1.35 ± 0.59	0.00 ± 0.00	0.18 ± 0.25	0.01 ± 0.01	1.38 ± 0.66	0.06 ± 0.03	25.10 ± 4.16
Sheep										
Dor	0.12 ± 0.23	0.01 ± 0.06	0.09 ± 0.15	0.79 ± 0.64	0.04 ± 0.10	0.10 ± 0.15	0.00 ± 0.01	0.84 ± 0.62	0.03 ± 0.02	32.2 ± 7.39
Pla	0.04 ± 0.13	0.00 ± 0.00	0.13 ± 0.16	0.83 ± 0.48	0.29 ± 0.44	0.13 ± 0.16	0.01 ± 0.01	1.12 ± 0.62	0.05 ± 0.03	25.8 ± 6.34
Med	0.13 ± 0.14	0.00 ± 0.00	0.13 ± 0.22	0.92 ± 0.68	0.00 ± 0.00	0.13 ± 0.22	0.01 ± 0.01	0.92 ± 0.68	0.03 ± 0.02	25.5 ± 8.65
Lat	0.07 ± 0.13	0.04 ± 0.10	0.15 ± 0.26	1.76 ± 1.00	0.00 ± 0.00	0.19 ± 0.33	0.02 ± 0.03	1.18 ± 1.08	0.13 ± 0.11	17.3 ± 5.37
Deer										
Dor	0.32 ± 0.36	0.01 ± 0.07	0.29 ± 0.39	1.56 ± 1.22	0.11 ± 0.23	0.31 ± 0.44	0.01 ± 0.01	1.73 ± 1.39	0.06 ± 0.12	35.45 ± 15.96
Pla	0.39 ± 0.37	0.00 ± 0.00	0.40 ± 0.42	1.60 ± 1.10	0.15 ± 0.27	0.44 ± 0.42	0.01 ± 0.01	1.93 ± 1.18	0.06 ± 0.04	34.78 ± 9.29
Med	0.10 ± 0.20	0.00 ± 0.00	0.30 ± 0.37	1.31 ± 0.87	1.31 ± 0.06	0.28 ± 0.37	0.02 ± 0.02	1.40 ± 0.94	0.08 ± 0.05	20.75 ± 8.49
Lat	0.20 ± 0.25	0.00 ± 0.00	0.28 ± 0.37	1.43 ± 0.65	0.01 ± 0.06	0.30 ± 0.36	0.02 ± 0.03	1.52 ± 0.70	0.17 ± 0.16	12.96 ± 6.40

Calcanei data summary of osteon variants in subgroups. OHI$_{(A)}$ = Osteon heterogeneity index (A) [(total atypical osteons)/(On.N/T.Ar); OHI$_{(DED)}$ = [(DED osteons)/(On.N/T.Ar)]; MC = multicanal.

Table 3. Paired comparisons among cortical quadrants in all species

	Connected group	Multicanal group	Elongate group
Horse radius	Cr<Cd, Cd>Lat, Cd>Med, Cr>Med	Cd>Lat, Cd>Med, Cr>Lat, Cr>Med	Cr>Lat,Cr>Med
Horse MC3	NS	NS	Dor>Pal
Deer calcaneus	Pla>Lat, Pla>Med, Dor>Med	NS	NS
Elk calcaneus	NS	Dor<Pla	NS
Horse calcaneus	Dor>Pla	Dor>Pla	NS
Sheep calcaneus	NS	Dor<Pla, Dor<Lat, Lat>Med	NS
	Drifting group	Zoned osteons	DED group
Horse radius	Cd>Lat	Cr<Cd, Cd>Lat, Cd>Med, Cr>Lat	Cd>Lat, Cd>Med, Cr>Lat, Cr>Med
Horse MC3	NS	NS	Dor>Med, Dor>Pal, Lat>Pal
Deer calcaneus	NS	Pla>Lat, Pla>Med	Pla>Lat, Pla>Dor
Elk calcaneus	NS	Dor>Pla	NS
Horse calcaneus	NS	NS	NS
Sheep calcaneus	NS	Dor<Pla, Pla>Lat, Pla>Med	NS
	$OHI_{(DED)}$	Total atypicals	$OHI_{(A)}$
Horse radius	Cr>Cd, Cr>Lat, Cr>Med	Cr<Cd, Cr>Lat and Med, Cd>Lat and Med	Cd>Lat, Cd>Med, Cr>Lat, Cr>Med
Horse MC3	Dor>Med, Dor>Pal, Lat>Pal, Lat>Med	NS	Dor>Pal
Deer calcaneus	Pla>Dor	NS	Pla<Lat, Dor<Lat, Dor>Med, Lat>Med
Elk calcaneus	NS	Dor>Pla, Pla<Lat	Dor<Pla
Horse calcaneus	NS	Dor>Pla, Pla<Lat	NS
Sheep calcaneus	NS	Dor<Lat	Dor>Pla, Dor<Lat, Lat>Med

Significant differences are indicated. For example, Cr > Cd represents a statistically significant ($p < 0.05$) cranial versus caudal difference. NS = Nonsignificant.

cies rejects hypothesis 1 since it is couched in a context of general applicability.

Hypothesis 2 states that analysis of *combined* data from all images of each cross section of the equine MC3s would show significantly more osteons that would increase interfacial complexity (i.e., DED group) when compared to the other bones. This is based on the idea that *generally increased* osteons of this type (especially increased numbers of elongated osteons) are associated with, and perhaps are adaptations for, torsional loading of the MC3 – which is attributed to shear stresses that are both prevalent/predominant and relatively more uniformly distributed across the cortex (when compared to bones that are habitually loaded in bending). This hypothesis was not supported (fig. 8).

Hypothesis 3 states that *endosteal regions* would have more prevalent 'atypical' osteons than the other intracortical regions, perhaps because endosteal regions experience lower strains or have increased metabolic influences associated with the nearby marrow. Data from the calcanei of all species do not support this hypothesis (fig. 9). In contrast, the endosteal region in the equine radii had significantly higher total 'atypical' osteons and $OHI_{(A)}$ [(total 'atypical' osteons)/(number of osteons/mm^2 bone)] than the periosteal region ($p < 0.05$ for both total 'atypical' osteons and $OHI_{(A)}$), but total 'atypical' osteons and $OHI_{(A)}$ were not significantly different between the endosteal and middle regions. The MC3s also had significantly higher $OHI_{(A)}$ in the endosteal than the periosteal region ($p < 0.05$), but the endosteal and middle regions were not significantly different. However, total 'atypical' osteons in the MC3s were significantly higher in the middle region than both the endosteal and periosteal regions ($p < 0.05$) (fig. 9).

Discussion

In general, the results of this study minimize, or eliminate, a role for variant osteon morphologies in drawing correlations between cortical bone microstructure and strain magnitude/mode distributions that occur in ha-

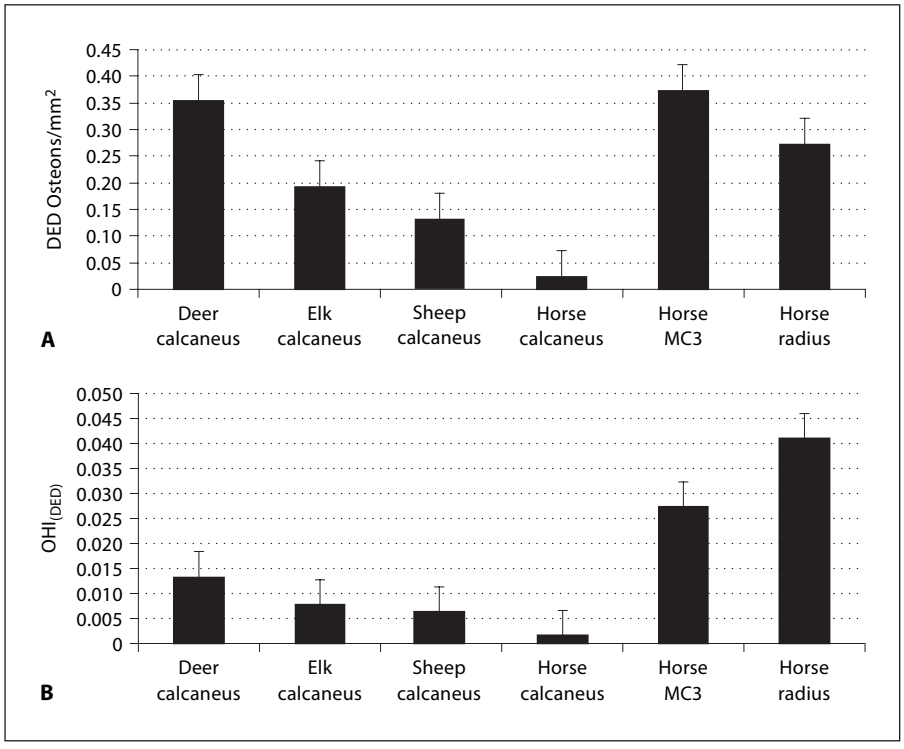

Fig. 8. Whole bone (all cross sections combined) data comparing all six bones: DED osteons (drifting, elongate group, and doublet-connected osteons) (**A**) and the $OHI_{(DED)}$ (**B**). **A** Note that the mean whole-bone DED osteon data for the MC3 (combined data from all octant cross sections) are higher than the horse calcaneus ($p = 0.06$), sheep calcaneus ($p = 0.08$) and the elk calcaneus (0.10). p values of $0.05 < p \leq 0.10$ are considered statistical trends. **B** Note that although the mean whole-bone $OHI_{(DED)}$ data for the MC3 (combined data from all octants) are higher than all calcanei, the comparison to the horse calcaneus ($p = 0.1$) is the only one close to being statistically significant.

Table 4. Correlations of some atypical osteon categories with On.Ar/T.Ar, NREs and CFO

	Deer calcaneus	Elk calcaneus	Horse calcaneus	Sheep calcaneus	Horse MC3	Horse radius
TAO versus						
On.Ar/T.Ar	r = 0.249[b]	r = 0.311[b]	r = –0.307[a]	r = 0.214	r = 0.241[b]	r = 0.490[b]
NREs	r = –0.011	r = –0.243	r = –0.243	r = 0.202	r = –0.072	r = 0.026
CFO	r = –0.283	NA	NA	NA	r = –0.072	r = 0.172[a]
$OHI_{(A)}$ versus						
On.Ar/T.Ar	r = –0.271[b]	r = 0.177	r = 0.177	r = –0.040	r = 0.035[b]	r = –0.262[b]
NREs	r = –0.090	r = –0.314[b]	r = –0.314[b]	r = 0.117	r = –0.051	r = 0.082
CFO	r = 0.508[b]	NA	NA	NA	r = –0.277[b]	r = 0.049
DED versus						
On.Ar/T.Ar	r = 0.191[a]	r = 0.036[a]	r = 0.114	r = –0.015	r = 0.076	r = 0.115
NREs	r = 0.038[a]	r = 0.036	r = 0.033	r = –0.283[a]	r = –0.059	r = 0.171[a]
CFO	r = –0.290	NA	NA	NA	r = –0.004	r = –0.014
$OHI_{(DED)}$ versus						
On.Ar/T.Ar	r = –0.128	r = 0.273	r = 0.058	r = –0.161	r = –0.288	r = –0.159[a]
NREs	r = –0.017	r = –0.023[a]	r = 0.057	r = –0.220	r = –0.047	r = 0.155[a]
CFO	r = 0.251	NA	NA	NA	r = –0.074	r = –0.061

Correlations of total atypical osteons (TAO, n/mm^2) and DED group osteons (drifting, elongate group, and doublet-connected osteons) with percent secondary bone [(On.Ar/T.Ar)·100], new remodeling events (NREs) and predominant collagen fiber orientation (CFO) in all cortical locations. [a] $0.01 < p < 0.05$; [b] $p < 0.01$. $OHI_{(A)}$ = Osteon heterogeneity index (A) [(TAO)/(On.N/T.Ar)]; DED = DED group osteons; $OHI_{(DED)}$ = [(DED osteons)/(On.N/T.Ar)]; NA = not applicable.

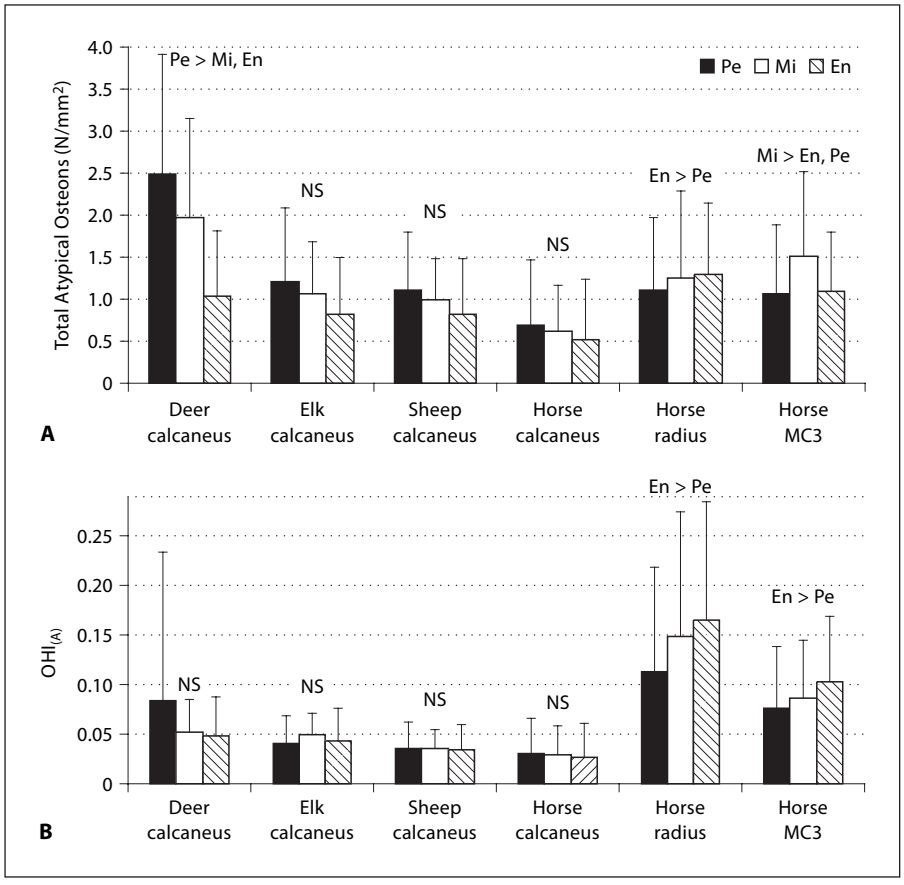

Fig. 9. Data comparing cortical regions (Pe, Mi, En) of all six bones: comparisons of total 'atypical' osteons (**A**) and comparisons of the OHI with respect to all osteons: $OHI_{(A)}$ = (total 'atypical' osteons)/(number of osteons/mm^2 bone) (**B**). NS = Nonsignificant; Pe = periosteal; Mi = middle; En = endosteal; Calc. = calcaneus. Statistics (example): En > Pe represents a statistically significant ($p < 0.05$) endosteal vs. periosteal difference.

bitual bending or torsion. Additionally, the results, which are mostly negative, strengthen our motivation to find other microstructural/ultrastructural characteristics (discussed below) that are more reliable for inferring the presence of these loading histories. Correlations between these osteon variants and habitual 'tension', 'tension/shear', 'compression', and neutral axis ('shear') regions were also poor even when considering potential influences of total (typical + atypical) osteon density, remodeling activity, and specific osteonal groupings. However, these negative results were *not* expected because there are data suggesting that some of these osteon morphologic variants might restrict microdamage formation/propagation by modifying the complexity of cement line interfaces in these habitual loading environments. One possible avenue for future investigations that are aimed at examining a putative role for osteonal microstructural interfaces in adaptive 'toughening' is to apply a method for calculating/estimating total cement line length per unit of bone area. Recent studies suggest that this may provide a better way for determining how cement line interfaces correlate with the micromechanical behavior of bone [Gibson et al., 2006].

A limitation of our study that belies the theoretical framework of our analysis is the possibility that the 'tension', 'shear', and 'compression' discriminators are not sufficiently distinct. Even though in vivo or rigorous ex vivo (deer calcaneus) strain data have been reported for all of the bone types that were used in the present study (fig. 6, 7), the equine MC3 is the only bone that we examined that has had intracortical strains estimated in vivo using finite element analyses based on data from more than two rosette strain gauges [Gross et al., 1992]. Until similar rigorous analyses are conducted on the equine radius and equine and artiodactyl calcanei, the hypotheses examined in the present study can only be considered indirectly. An additional limitation of this study includes the paucity of experimental fracture toughness data in the putative 'tension', 'compression', and 'shear' cortices of the bones examined. Our hypotheses were, in part, based on the idea that the emergence of osteonal interfacial complexity during normal development produc-

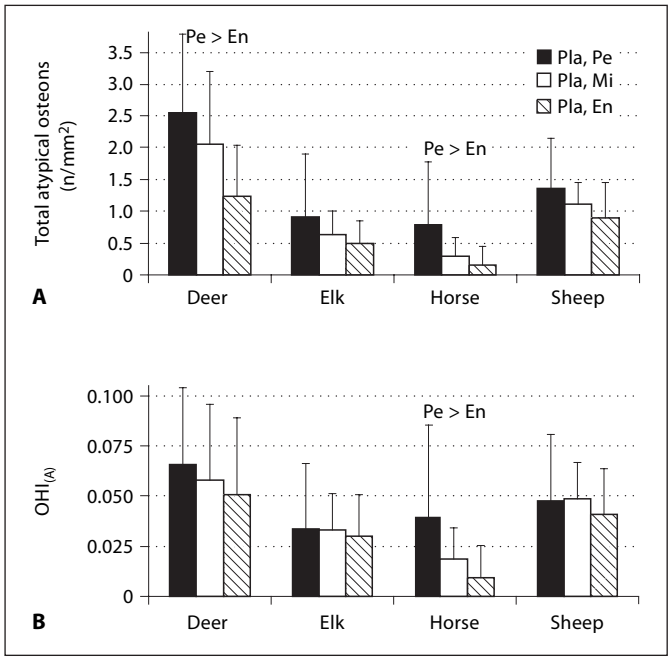

Fig. 10. Cortical region (Pe, Mi, En) comparisons in plantar (Pla) calcaneal cortices of total 'atypical' osteons (**A**) and comparisons of the OHI with respect to all osteons: $OHI_{(A)}$ = (total 'atypical' osteons)/(number of osteons/mm^2 bone) (**B**). NS = Nonsignificant; Pla, Pe = plantar periosteal; Pla, Mi = plantar middle; Pla, En = plantar endosteal. Pe > En represents a statistically significant ($p < 0.05$) periosteal vs. endosteal difference.

es regional 'toughening' for these prevalent/predominant strain modes. Because rigorous mechanical testing studies are needed to directly address this issue [Joo et al., 2004; Vashishth, 2004; Ural and Vashishth, 2006; Skedros et al., 2006a], the possibility that one or more characteristics of osteonal or collagen/lamellar organization strongly correlate with toughening remains an open question. Finally, sample size limitations may have reduced statistical power to a level below what would be needed to detect some of the hypothesized regional variations. However, using the methods and data from the present study, a retrospective power analysis for detecting osteons that increase interfacial complexity (the DED group) in all bones suggests that approximately 5,000 bones would be needed to detect >5% difference ($\alpha < 0.05$; $p = 0.9$; $\beta = 0.1$) even when allowing a generous error of ± 0.01. Additionally, using these parameters, approximately 5,000 bones would be needed to detect a significant association of 'elongated osteons' with a neutral axis ('shear') region. In view of these analyses, it would be predicted that the regional variations in the population densities of these osteonal variants would still be so small, or inconsistent, that they would be highly *un*reliable for inferring the presence of a history of habitual bending in most bone types.

Some important additional observations made in the present study included the very infrequent occurrence of drifting and zoned/embedded osteons. One explanation for this is that since the bones in the present study are from the appendicular skeleton, they are not a significant source for remodeling-mediated calcium mobilization (e.g., in contrast to ribs where drifting and zoned/embedded osteons might be more important in this regard). In addition, the rarity of drifting osteons in our specimens may be because they are more common in younger animals [Johnson, 1964]. Knese and Titschak [1962] reported that drifting osteons were <1% of all osteons in principal metacarpals of pigs and wild boars. In contrast, Knese et al. [1954b] found drifting osteons to be the *most predominant* osteon variant (roughly 10% of the quantified osteons) in appendicular bones (femur, tibia, fibula, and radius) of a 43-year-old human male. An increased prevalence of drifting osteons in the human skeleton, and perhaps in the skeletons of other anthropoids, may reflect interspecies differences. The biomechanical/metabolic importance and causal bases for the existence of these 'unusual' osteons have not been resolved [Currey, 2002; Rauch et al., 2007]. Zoned/embedded osteons may also be more prevalent in aged animals, which were not included in our samples. Although our tissues were not adequate for evaluating potential associations of zoned/embedded osteons with systemic/metabolic stress, we postulated that these osteonal variants might be most prevalent in the relatively metabolically active endosteal regions or in the low-strain plantar calcaneal cortices [Skedros et al., 2001]. These hypotheses, however, are not supported by the data, including our additional observations within the plantar calcaneal cortices (fig. 10).

Interspecies and intraspecies differences in the prevalence and distributions of typical and 'atypical' osteons might be strongly influenced by differences in bone formation rates and developmental constraints [Céspedes Diaz and Rajtovà, 1975; de Ricqlès et al., 1991; Ferretti et al., 1999]. A poignant example includes the rarity of drifting osteons in the bones examined herein versus the relatively high prevalence reported in human bones. Another confounding variable is suggested by the observation that increased osteonal interconnections could simply result from new osteons arising out of old osteons, which reflects the fact that osteons tend to primarily form in a nonpioneering fashion (i.e., they tend to form in direct

association with existing secondary osteons) [Tappen, 1977; Martin and Burr, 1989]. We had speculated that interconnections would therefore also be more prevalent in regions where remodeling rates are relatively elevated (e.g., plantar calcaneal cortices), which might suggest that the resulting increased interfacial complexity is an epiphenomenon in the context of mechanical adaptation. Even if this presumption is correct, the locations where old and new canals become confluent might be difficult to detect without examining multiple serial sections (fig. 5). A relatively broad range of remodeled bone might also be required for showing stronger correlations. These limitations of our study – few cross sections analyzed, and a rather narrow range of percent secondary bone area – may explain why higher correlations were not found between amount of remodeling and connected/multiple-canal osteons.

The prevalence of some osteonal variants could also be strongly correlated with, and hence confounded by, regional variations in mean tissue age and/or the cortical envelope in which these analyses are conducted [Epker and Frost, 1965; Rauch et al., 2007]. Age-related cortical modeling and remodeling drifts can produce variations in tissue age between cortices in the same cross section [Amprino and Marotti, 1964; Frost, 1987; Martin and Burr, 1989, p. 53]. Thus, in some bones, regional variations in secondary osteon population density and/or some osteonal morphologic characteristics may have more to do with growth-related modeling and remodeling drifts than with demands of mechanical loading [Amprino and Sisto, 1946; Enlow, 1962, 1963; Oyen and Russell, 1982; de Ricqlès et al., 1991; McMahon et al., 1995].

Recent investigations have shown that there are mechanically relevant distinctions in osteon morphologies that cannot be seen when using conventional light microscopy, backscattered electron imaging, or microradiography [Martin et al., 1996a; Hiller et al., 2003; Skedros et al., 2006b]. These include variations in osteon lamellar organization that are seen as birefringent patterns in circularly polarized light – 'hooped' osteons (with bright, highly transverse, peripheral lamellae) versus alternating osteons [with alternating bright and dark (longitudinal) lamellae], which can differentially influence fatigue and toughness behaviors in tension, compression, and shear. Additional characteristics that might reveal stronger correlations in the context of hypotheses examined in the present study include: (1) measures of three-dimensional osteonal complexities that require three-dimensional reconstruction to adequately resolve (e.g., osteon interconnections, interdigitations, and three-dimensional orientation) [Stout et al., 1999; Mohsin et al., 2002; Nalla et al., 2005] and (2) distributions in other matrix characteristics that might be mediated by osteon formation, including collagen molecular cross-links and dissociations of mineral/collagen alignment [Burr, 2002; Skedros et al., 2006c].

Conclusions

Regional variations in the prevalence of osteon variants were not consistently associated with habitual loading histories in various bone types. Correlations between the population densities of osteon variants and what we considered as habitual 'tension', 'tension/shear', 'compression', and neutral axis ('shear') regions were also poor, even when considering the influences of population densities of all secondary osteons, remodeling activity, and specific groupings of the osteon variants. Spatial variations in these osteon variants, therefore, do not appear to be generally useful for inferring relatively increased remodeling rates/metabolism or load history characterized by torsion or bending. Further studies aimed at clarifying the reliability of using other microstructural/ultrastructural characteristics in this context are warranted since skeletal morphologists often analyze bones where ethical considerations preclude in vivo strain gauge measurements or obtaining these data is difficult or impossible, including some anthropoid bones or bone regions, exhumed skeletons, and fossils. New avenues of research suggest that regional variations in predominant collagen fiber orientation and/or secondary osteons with specific lamellar organization (as seen in circularly polarized light) may prove to be sufficiently sensitive for interpreting loading histories in bones where obtaining in vivo strain data is difficult or not possible.

Acknowledgements

The authors thank Roy Bloebaum and the Salt Lake City Veterans Administration Bone and Joint Research Laboratory for providing some of the technical equipment and support used for this study. The authors also thank Aaron Young, Mark Mason, and Mark Nelson for their technical work, Kerry Matz for illustrations, Brian Libbey for library services, and Christian Sybrowsky and two anonymous reviewers for their criticisms. The authors also thank Alex Robling for suggesting that we further investigate the prevalence of drifting osteons. Funding for this work was provided by the Department of Veterans Affairs Medical Research Funds, the Utah Bone and Joint Center, Salt Lake City, Utah, and Orthopaedic Research and Education Foundation grant 01-024.

Appendix

Descriptions of Osteon Morphologies (fig. 4), *Mechanical/Metabolic Implications, and Related Issues*

Based on spatial/temporal remodeling activities reported in mature dog fibulae [Enneking et al., 1972], which presumably receive cranial-caudal bending, Brand concluded that the morphology and distributions of secondary osteons appear to be 'infinitely variable …' [Brand, 1992, p. 108]. He considered such microstructural variability as inconsequential and inconsistent with any view of 'spatial coordination and adaptability' or 'order and concordance at a higher level of bone organization'. Distributions of secondary osteons in diaphyses of modern human and canine femora, and sheep, human and canine tibiae also do *not* clearly reflect their nonuniform strain distributions [Moyle et al., 1978; Martin et al., 1980; Skedros, 2001; Goldman et al., 2003; Drapeau and Streeter, 2006]. In contrast to these suggestions of randomness or quasi randomness in secondary osteon distributions, qualitative microscopic observations of bones habitually loaded in bending suggest that the more highly strained 'compression' cortices tend to have higher numbers of secondary osteons [Lanyon and Bourn, 1979; Lanyon et al., 1979; Bouvier and Hylander, 1981; Carter et al., 1981; Gies and Carter, 1982; Portigliatti Barbos et al., 1983]. Secondary osteon population densities have also been shown to be significantly greater in quantitative studies of habitual 'compression' versus 'tension' cortices of equine and sheep radii, and sheep, deer, elk, and horse calcanei [Mason et al., 1995; Skedros et al., 1997; Sorenson et al., 2004]. Variations in the cross-sectional area of individual secondary osteons has also been shown to be an unreliable characteristic for interpreting load history in the contexts of habitual bending and torsion, and in other general biomechanical contexts [Skedros et al., 1994b; Mason et al., 1995; Skedros et al., 1996; Skedros, 2001; Pfeiffer et al., 2006]. In some cases the population densities of secondary osteons and/or differences in the mean cross-sectional area or shape of individual osteons have been reported as useful for distinguishing interspecies differences, and age-, behavior-, and/or gender-related differences between individuals within the same species [Schaffler and Burr, 1984; Abbott et al., 1996; Mulhern and Van Gerven, 1997; Hidaka et al., 1998; Dittmann, 2003; Mulhern and Ubelaker, 2003; Havill, 2004; Urbanová and Novotný, 2005; Martiniaková et al., 2006]. In the perspective of these studies, we speculated that correlations between osteonal morphology with local load history could have been consistently detected in these previous studies if regional variations in the osteon *variants* examined in the present study (and described below) had been considered as possible adaptations for regional 'toughening' in the 'tension', 'compression', and 'shear' regions of bones habitually loaded in bending or torsion.

The osteon characteristics examined in the present study have been described and interpreted in various mechanical, metabolic, and/or age-related contexts. In torsionally loaded bones such as diaphyses of human and canine femora, equine MC3s, and sheep tibiae, some investigators have reported a relatively high prevalence of obliquely oriented secondary osteons [Sinelnikov, 1937; Cohen and Harris, 1958; Lanyon and Bourn, 1979; Lanyon et al., 1979; Saito, 1984; Petrtýl et al., 1996]. In transverse cross sections these obliquely oriented osteons should appear as variants that we classify as 'elongated osteons'. Elongated osteons have also been reported as relatively prevalent in medial/lateral (neutral axis or 'shear') cortices of sheep, deer, elk, and horse calcanei [Skedros, 1994; Skedros et al., 1994a, 1997; Sorenson et al., 2004]. In some cases, however, regional variations in the prevalence of osteonal elongation and other related osteonal morphologic characteristics (e.g., connected, dumbbell, and dumbbell connected) might not be biomechanically adaptive. For example, these variations might also be influenced by local metabolism (see below).

In diaphyses of modern adult human femora, Bell et al. [2001] observed clusters of secondary osteons that they called 'clustered' osteons or 'superosteons'. Such clusters can lead to 'giant osteons' and connected osteons, which are characterized by the merging of central canals. Both connected and giant osteons contribute to increased porosity, but giant osteons are more strongly associated with aging [Power et al., 2003; Cooper et al., 2006]. Connected osteons and related osteon characteristics (e.g., dumbbell, elongated, and multiple canal) might also reflect furcates and/or anastomoses [Koltze, 1951; Cohen and Harris, 1958; Stout et al., 1999]. Additional osteon morphologies that might help to enhance local mechanical properties include variations in cross-sectional size and/or shape (e.g., dumbbell and elongated osteons), coupled with preferred collagen orientation [Pidaparti and Burr, 1992; Martin et al., 1996a; Skedros et al., 2004; Gibson et al., 2006].

Double-zoned (or embedded) osteons may be the result of 'intraosteonal remodeling' of an existing secondary osteon [Pankovich et al., 1974; Nyssen-Behets et al., 1994, 1996]. Such remodeling results in a new BMU forming within a relatively older osteon, which leaves the cement line of the older osteon unperturbed. However, when an embedded osteon mineralizes completely, its cement line (i.e., reversal line) can be confused with a hypermineralized ring or 'halo' (i.e., arrest or resting line) that represents the slowing or transient cessation of osteon closure. In modern adult human tibiae sectioned at mid-diaphysis (age range: 40–81 years), Kornblum and Kelly [1964] observed zoned osteons with three to four of these hypermineralized lamellar 'halos'. Although described as embedded osteons by some (see below), other investigators describe the refilling of the enlarged central canals with bone as double-zoned osteons. For example, in a study of modern human ribs (age range: 8–80 years), Pankovich et al. [1974] observed increased double-zoned osteons with age, reflecting a possible age-related increase in intraosteonal remodeling and/or the temporary cessation of osteonal infilling. This latter possibility is consistent with findings of Kornblum and Kelly [1964] in modern human tibiae where they suggested that these osteons reflect '… cessation of growth [osteon infilling] at one time …' (p. 807). Regardless of how they are produced, zoned/embedded osteons can result in mineralization heterogeneity (increased osteons that have lower mineralization on average) that can enhance toughness and fatigue life [Phelps et al., 2000; Gibson et al., 2006]. Martin and Burr [1989] suggest that intraosteonal remodeling may be a means for mobilizing calcium while minimizing deleterious effects on osteon-related mechanical properties. However, since zoned/embedded osteons are relatively infrequent in bones of healthy nonsenescent individuals, they may produce microscopic mineralization heterogeneity implicated in age-related fragility [Vajda and Bloebaum, 1999; Phelps et al., 2000; Currey, 2002].

Increased prevalence of zoned and embedded osteons might reflect systemic stress or changes in metabolic demands. For example, Richman et al. [1979] reported a high frequency of what we consider to be embedded osteons in the anterior femoral cortices of 51 Alaskan Eskimos (age range: 18 years to elderly) from

the late 1700s to early 1900s. These individuals typically consumed a high protein, meat diet, which can cause metabolic acidosis and hypercalciuria, resulting in the loss of bone mineral. They also suggested that starvation and high-fat diets, which result in ketone body production and the mobilization of calcium salts from bone to buffer the acidity, might yield more embedded osteons in some individuals. Other investigators argue that in some situations embedded osteons are the result of a degenerative process where a hypermineralized lamellar ring forms around the Haversian canal. It has been suggested that the excessive mineral deposition leads to necrosis of surrounding osteocytes. Nyssen-Behets et al. [1996] state that subsequently such '… hypermineralized lamellae may crumble down because of their excessive brittleness, giving rise to haversian canals with notched walls'. In turn these investigators suggest that the collapse of these brittle lamellae leads to the formation of bone *without* antecedent osteoclast activity (the 'second type' of resorption space described by Jaworski et al. [1972]) [Nyssen-Behets et al., 1994, 1996]. Regardless of how zoned/embedded osteons form, they are considered as 'double-zoned' osteons in the present study, reflecting our inability to confidently differentiate between them.

The drifting osteon is a highly unusual secondary osteon variant that may play a role in enhancing bone mechanical properties, especially toughness, by creating greater interfacial surfaces (cement lines) [Robling and Stout, 1999]. Johnson [1964, p. 585] described drifting osteons as 'geographic osteons', and Knese and Titschak [1962] described them as 'schalensteons' (their lamellae resemble the grooved patterns of a mussel shell). Epker and Frost [1965] suggested that in human ribs this osteon variant consistently drifts toward the endosteum (i.e., probably bone with greatest mean tissue age, hence highest mineralization) thereby maximizing available mineral for homeostatic purposes. According to Robling and Stout [1999], Coutelier [1976] also suggested that the primary stimulus for drifting osteons is mineral homeostasis, while mechanical influences are secondary consequences. But this interpretation is controversial [Robling and Stout, 1999]. Although drifting osteons are thought to primarily occur in young bone, Robling and Stout [1999, unpubl. data] observed them in cross sections of limb long bones from modern humans in 'every decade of life'.

References

Abbott, S., E. Trinkaus, D.B. Burr (1996) Dynamic bone remodeling in later pleistocene fossil hominids. Am J Phys Anthropol *99:* 585–601.

Akkus, O., F. Adar, M.B. Schaffler (2004) Age-related changes in physicochemical properties of mineral crystals are related to impaired mechanical function of cortical bone. Bone *34:* 443–453.

Akkus, O., D.F. Knott, K.J. Jepsen, D.T. Davy, C.M. Rimnac (2003) Relationship between damage accumulation and mechanical property degradation in cortical bone: microcrack orientation is important. J Biomed Mater Res *65A:* 482–488.

Albrektsson, T., C. Johansson (1991) Quantified bone tissue reactions to various metallic materials with reference to the so-called osseointegration concept; in Davies, J.E. (ed): The Bone-Biomaterial Interface. Toronto, University of Toronto Press, pp 357–363.

Amprino, R., G. Marotti (1964) A topographic quantitative study of bone formation and reconstruction; in Blackwood, H. (ed): Bone and Tooth. London, Pergamon Press, pp 21–33.

Amprino, R., L. Sisto (1946) Analogies et différences de structure dans les différentes régions d'un même os. Acta Anat *2:* 202–214.

Anderson, W.E., J.G. Skedros (2005) Comparative analysis of confocal and light microscopy for detecting in vivo microdamage in wild and domesticated animals. J Bone Miner Res *20:* S324.

Bell, K.L., N. Loveridge, J. Reeve, C.D. Thomas, S.A. Feik, J.G. Clement (2001) Super-osteons (remodeling clusters) in the cortex of the femoral shaft: influence of age and gender. Anat Rec *264:* 378–386.

Biewener, A.A., J.E.A. Bertram (1993) Mechanical loading and bone growth in vivo; in Hall, B.K. (ed): Bone. Boca Raton, CRC Press, vol 7: Bone Growth – B, pp 1–36.

Biewener, A.A., K.P. Dial (1995) In vivo strain in the humerus of pigeons *(Columba livia)* during flight. J Morphol *225:* 61–75.

Biewener, A.A., S.M. Swartz, J.E.A. Bertram (1986) Bone modeling during growth: dynamic strain equilibrium in the chick tibiotarsus. Calcif Tissue Int *39:* 390–395.

Biewener, A.A., J. Thomason, A. Goodship, L.E. Lanyon (1983a) Bone stress in the horse forelimb during locomotion at different gaits: a comparison of two experimental methods. J Biomech *16:* 565–576.

Biewener, A.A., J. Thomason, L.E. Lanyon (1983b) Mechanics of locomotion and jumping in the forelimb of the horse *(Equus)*: in vivo stress developed in the radius and metacarpus. J Zool Lond *201:* 67–82.

Bousson, V., A. Meunier, C. Bergot, E. Vicaut, M.A. Rocha, M.H. Morais, A.M. Laval-Jeantet, J.D. Laredo (2001) Distribution of intracortical porosity in human midfemoral cortex by age and gender. J Bone Miner Res *16:* 1308–1317.

Bouvier, M., W.L. Hylander (1981) Effect of bone strain on cortical bone structure in macaques *(Macaca mulatta)*. J Morphol *167:* 1–12.

Boyce, T.M., D.P. Fyhrie, M.C. Glotkowski, E.L. Radin, M.B. Schaffler (1998) Damage type and strain mode associations in human compact bone bending fatigue. J Orthop Res *16:* 322–329.

Boyde, A., C.M. Riggs (1990) The quantitative study of the orientation of collagen in compact bone slices. Bone *11:* 35–39.

Brand, R.A. (1992) Autonomous informational stability in connective tissues. Med Hypotheses *37*: 107–114.

Burr, D.B. (2002) The contribution of the organic matrix to bone's material properties. Bone *31:* 8–11.

Burr, D.B., R.B. Martin, M.B. Schaffler, E.L. Radin (1985) Bone remodeling in response to in vivo fatigue microdamage. J Biomech *18:* 189–200.

Burr, D.B., M.B. Schaffler, R.G. Frederickson (1988) Composition of the cement line and its possible mechanical role as a local interface in human compact bone. J Biomech *21:* 939–945.

Burstein, A.H., D.T. Reilly, M. Martens (1976) Aging of bone tissue: mechanical properties. J Bone Joint Surg *58-A:* 82–86.

Carter, D.R., W.E. Caler, D.M. Spengler, V.H. Frankel (1981) Fatigue behavior of adult cortical bone: the influence of mean strain and strain range. Acta Orthop Scand *52:* 481–490.

Carter, D.R., W.C. Hayes (1977a) Compact bone fatigue damage: residual strength and stiffness. J Biomech *10:* 325–337.

Carter, D.R., W.C. Hayes (1977b) The compressive behavior of bone as a two-phase porous structure. J Bone Joint Surg Am *59:* 954–962.
Céspedes Diaz, C.M., V. Rajtovà (1975) Comparative study of lamellar bone in some carnivora. Folia Morphol (Praha) *23:* 221–229.
Cohen, J., W.H. Harris (1958) The three-dimensional anatomy of haversian systems. J Bone Joint Surg Am *40-A:* 419–434.
Coleman, J.C., R.T. Hart, I. Owan, Y. Tankano, D.B. Burr (2002) Characterization of dynamic three-dimensional strain fields in the canine radius. J Biomech *35:* 1677–1683.
Cooper, D., C. Thomason, J. Clement, B. Hallgrimsson (2006) Three-dimensional microcomputed tomography imaging of basic multicellular unit-related resorption spaces in human cortical bone. Anat Rec A Discov Mol Cell Evol Biol *288:* 806–816.
Coutelier, L. (1976) Le remaniement interne de l'os compact chez l'enfent. Bull Assoc Anat *60:* 95–110.
Currey, J.D. (2002) Bones: Structure and Mechanics. Princeton, Princeton University Press, p 436.
Da Costa Gómez, T.M., J.G. Barrett, S.J. Sample, C.L. Radtke, V.L. Kalscheur, Y. Lu, M.D. Markel, E.M. Santschi, M.C. Scollay, P. Muir (2005) Up-regulation of site-specific remodeling without accumulation of microcracking and loss of osteocytes. Bone *37:* 16–24.
Demes, B., J.T. Stern, Jr., M.R. Hausman, S.G. Larson, K.J. McLeod, C.T. Rubin (1998) Patterns of strain in the macaque ulna during functional activity. Am J Phys Anthropol *106:* 87–100.
de Ricqlès, A., F.J. Meunier, L. Castanet, H. Francillon-Vieillot (1991) Comparative microstructure of bone; Hall, B.K. (ed): Bone. Boca Raton, CRC Press, vol 3: Bone Matrix and Bone Specific Products, pp 1–78.
Diab, T., D. Vashishth (2007) Morphology, localization and accumulation of in vivo microdamage in human cortical bone. Bone *40:* 612–618.
Dittmann, K. (2003) Histomorphometrische Untersuchung der Knochen-Mikrostruktur von Primaten und Haustieren mit dem Ziel der Speziesidentifikation unter Berücksichtigung von Domestikationseffekten. Anthrop Anz *61:* 175–188.
Drapeau, M.S.M., M.A. Streeter (2006) Modeling and remodeling responses to normal loading in the human lower limb. Am J Phys Anthropol *129:* 403–409.
Drucker, D.C. (1967) Introduction to Mechanics of Deformable Solids. New York, McGraw Hill.
Ehrlich, P.J., L.E. Lanyon (2002) Mechanical strain and bone cell function: a review. Osteoporos Int *13:* 688–700.
Emmanual, J., C. Hornbeck, R.D. Bloebaum (1987) A polymethyl methacrylate method for large specimens of mineralized bone with implants. Stain Tech *62:* 401–410.
Enlow, D.H. (1962) Functions of the Haversian system. Am J Anat *110:* 269–305.
Enlow, D.H. (1963) Principles of Bone Remodeling. Springfield, Charles C. Thomas, pp 1–131.
Enneking, W.F., H. Burchardt, J.J. Puhl, J. Thornby (1972) Temporal and spatial activity in mirror segments of mature dog fibulae. Calcif Tissue Res *9:* 283–295.
Epker, B.N., H.M. Frost (1965) The direction of transverse drift of actively forming osteons in human rib cortex. J Bone Joint Surg Am *47:* 1211–1215.
Ferretti, M., M.A. Muglia, F. Remaggi, V. Canè, C. Palumbo (1999) Histomorphometric study on the osteocyte lacuno-canalicular network in animals of different species. II. Parallel-fibered and lamellar bones. Ital J Anat Embryol *104:* 121–131.
Fritton, S.P., K.J. McLeod, C.T. Rubin (2000) Quantifying the strain history of bone: spatial uniformity and self-similarity of low-magnitude strains. J Biomech *33:* 317–325.
Frost, H.M. (1987) Secondary osteon populations: an algorithm for determining mean bone tissue age. Yearb Phys Anthropol *30:* 221–238.
George, W.T., D. Vashishth (2005) Damage mechanisms and failure modes of cortical bone under components of physiological loading. J Orthop Res *23:* 1047–1053.
Gere, J.M., S.P. Timoshenko (1984) Mechanics of Materials. Boston, PWS-Kent, p 762.
Gibbons, J. (1976) Nonparametric Methods for Quantitative Analysis. Holt, Rinehart & Winston, pp 1–463.
Gibson, V.A., S.M. Stover, J.C. Gibeling, S.J. Hazelwood, R.B. Martin (2006) Osteonal effects on elastic modulus and fatigue life in equine bone. J Biomech *39:* 217–225.
Gies, A.A., D.R. Carter (1982) Experimental determination of whole long bone sectional properties. J Biomech *15:* 297–303.
Goldman, H.M., T.G. Bromage, C.D. Thomas, J.G. Clement (2003) Preferred collagen fiber orientation in the human mid-shaft femur. Anat Rec *272A:* 434–445.
Gross, T.S., K.J. McLeod, C.T. Rubin (1992) Characterizing bone strain distribution in vivo using three triple rosette strain gauges. J Biomech *25:* 1081–1087.
Havill, L.M. (2004) Osteon remodeling dynamics in *Macaca mulatta:* normal variation with regard to age, sex, and skeletal maturity. Calcif Tissue Int *74:* 95–102
Hidaka, S., M. Matsumoto, S. Ohsako, Y. Toyoshima, H. Nishinakagawa (1998) A histometrical study on the long bones of raccoon dogs, *Nyctereutes procyonoides* and badgers, *Meles meles*. J Vet Med Sci *60:* 323–326.
Hiller, L.P., S.M. Stover, V.A. Gibson, J.C. Gibeling, C.S. Prater, S.J. Hazelwood, O.C. Yeh, R.B. Martin (2003) Osteon pullout in the equine third metacarpal bone: effects of ex vivo fatigue. J Orthop Res *21:* 481–488.
Jaworski, Z.F., P. Meunier, H.M. Frost (1972) Observations on two types of resorption cavities in human lamellar cortical bone. Clin Orthop *83:* 279–285.
Johnson, L. (1964) Morphologic analysis in pathology: the kinetics of disease and general biology of bone; in Frost, H.M. (ed): Bone Biodynamics. Boston, Little, Brown, pp 543–654.
Joo, W., K.J. Jepsen, D.T. Davy (2004) Complex cross-modal effects of damage on cortical bone properties. Trans Orthop Res Soc *29:* 515.
Kalmey, J.K., C.O. Lovejoy (2002) Collagen fiber orientation in the femoral necks of apes and humans: do their histological structures reflect differences in locomotor loading. Bone *31:* 327–332.
Knese, K.H. (1979) Stützgewebe und Skelettsystem. Handb Mikrosk Anat D Menschen 2. Die Gewebe. Berlin, Springer.
Knese, K.H., I. Ritschl, D. Voges (1954a) Quantitative studies on osteon distribution in the extremital skeleton of a 43 year old man. Z Zellforsch Mikrosk Anat *40:* 519–570.
Knese, K.H., S. Titschak (1962) Untersuchungen mit Hilfe des Lochkartenverfahrens über die Osteonstruktur von Haus- und Wildschweinknochen sowie Bemerkungen zur Baugeschichte des Knochengewebes. Jahrb Morphol Mikrosk Anat *102:* 337–459.
Knese, K.H., D. Voges, I. Ritschl (1954b) Studies on osteon and lamellar forms in extremital skeleton in adult. Z Zellforsch Mikrosk Anat *40:* 323–360.
Koltze, H. (1951) Studie zur äusseren Form der Osteone. Z Anat Entwicklungsgesch *115:* 585–596.
Kornblum, S.S., P.J. Kelly (1964) The lacunae and haversian canals in tibial cortical bone from ischemic and non-ischemic limbs. A comparative microradiographic study. J Bone Joint Surg Am *46:* 797–810.
Lanyon, L.E. (1987) Functional strain in bone tissue as an objective, and controlling stimulus for adaptive bone remodelling. J Biomech *20:* 1083–1093.
Lanyon, L.E., D.G. Baggott (1976) Mechanical function as an influence on the structure and form of bone. J Bone Joint Surg *58-B:* 436–443.
Lanyon, L.E., S. Bourn (1979) The influence of mechanical function on the development and remodeling of the tibia: an experimental study in sheep. J Bone Joint Surg *61-A:* 263–273.
Lanyon, L.E., P.T. Magee, D.G. Baggott (1979) The relationship of functional stress and strain to the processes of bone remodeling: an experimental study on the sheep radius. J Biomech *12:* 593–600.
Lieberman, D.E., O.M. Pearson, J.D. Polk, B. Demes, A.W. Crompton (2003) Optimization of bone growth and remodeling in response to loading in tapered mammalian limbs. J Exp Biol *206:* 3125–3138.

Lieberman, D.E., J.D. Polk, B. Demes (2004) Predicting long bone loading from cross-sectional geometry. Am J Phys Anthropol *123:* 156–171.
Martin, R.B. (2003a) Fatigue damage, remodeling, and the minimization of skeletal weight. J Theor Biol *220:* 271–276.
Martin, R.B. (2003b) Fatigue microdamage as an essential element of bone mechanics and biology. Calcif Tissue Int *73:* 101–107.
Martin, R.B., D.B. Burr (1989) Structure, Function and Adaptation of Compact Bone. New York, Raven Press, pp 1–275.
Martin, R.B., D.B. Burr, N.A. Sharkey (1998) Skeletal Tissue Mechanics. New York, Springer, pp 1–392.
Martin, R.B., V.A. Gibson, S.M. Stover, J.C. Gibeling, L.V. Griffin (1996a) Osteonal structure in the equine third metacarpus. Bone *19:* 165–171.
Martin, R.B., P.V. Mathews, S.T. Lau, V.A. Gibson, S.M. Stover (1996b) Collagen fiber organization is related to mechanical properties and remodeling in equine bone. A comparison of two methods. J Biomech *29:* 1515–1521.
Martin, R.B., P.V. Mathews, S.T. Lau, V.A. Gibson, S.M. Stover (1996c) Use of circularly vs. plane polarized light to quantify collagen fiber orientation in bone. Trans Orthop Res Soc *21:* 606.
Martin, R.B., J.C. Pickett, S. Zinaich (1980) Studies of skeletal remodeling in aging men. Clin Orthop *149:* 268–282.
Martiniaková, M., B. Grosskopf, R. Omelka, M. Vondráková, M. Bauerová (2006) Differences among species in compact bone tissue microstructure of mammalian skeleton: use of discriminant function analysis for species identification. J Forensic Sci *51:* 1235–1239.
Mason, M.W., J.G. Skedros, R.D. Bloebaum (1995) Evidence of strain-mode-related cortical adaptation in the diaphysis of the horse radius. Bone *17:* 229–237.
McMahon, J.M., A. Boyde, T.G. Bromage (1995) Pattern of collagen fiber orientation in the ovine calcaneal shaft and its relation to locomotor-induced strain. Anat Rec *242:* 147–158.
Mohsin, S., D. Taylor, T.C. Lee (2002) Three-dimensional reconstruction of Haversian systems in ovine compact bone. Eur J Morphol *40:* 309–315.
Moyle, D.D., J.W. Welborn, 3rd, F.W. Cooke (1978) Work to fracture of canine femoral bone. J Biomech *11:* 435–440.
Mulhern, D.M., D.P. Van Gerven (1997) Patterns of femoral bone remodeling dynamics in a medieval Nubian population. Am J Phys Anthropol *104:* 133–146.
Mulhern, D.M., D.H. Ubelaker (2003) Histologic examination of bone development in juvenile chimpanzees. Am J Phys Anthropol *122:* 127–133.
Nalla, R.K., J.J. Kruzic, J.H. Kinney, R.O. Ritchie (2005) Mechanistic aspects of fracture and R-curve behavior in human cortical bone. Biomaterials *26:* 217–231.
Nelson, G.E., Jr., P.J. Kelly, L.F. Peterson, J.M. Janes (1960) Blood supply of the human tibia. Am J Orthop *42-A:* 625–636.
Nunamaker, D. (2001) Bucked shins in horses; in Burr, D.B., C. Milgrom (eds): Musculoskeletal Fatigue and Stress Fractures. Boca Raton, CRC Press, pp 203–219.
Nyssen-Behets, C., V. Arnould, A. Dhem (1994) Hypermineralized lamellae below the bone surface: a quantitative microradiographic study. Bone *15:* 685–689.
Nyssen-Behets, C., P.Y. Duchesne, A. Dhem (1996) Structural changes with aging in cortical bone of the human tibia. Gerontology *43:* 316–325.
O'Brien, F.J., D. Taylor, T.C. Lee (2003) Microcrack accumulation at different intervals during fatigue testing of compact bone. J Biomech *36:* 973–980.
Oyen, O.J., M.D. Russell (1982) Histogenesis of the craniofacial skeleton and models of facial growth; McNamara, J.A., Jr., D.S. Carlson, K.A. Ribbens (eds): The Effect of Surgical Intervention on Craniofacial Growth. Monograph No. 12. Craniofacial Growth Series. Ann Arbor, University of Michigan, pp 361–372.
Pankovich, A.M., D.J. Simmons, V.V. Kulkarni (1974) Zonal osteons in cortical bone. Clin Orthop *100:* 356–363.
Petrtýl, M., J. Hert, P. Fiala (1996) Spatial organization of Haversian bone in man. J Biomech *29:* 161–169.
Pfeiffer, S., C. Crowder, L. Harrington, M. Brown (2006) Secondary osteons and haversian canal dimensions as behavioral indicators. Am J Phys Anthropol *131:* 460–468.
Phelps, J.B., G.B. Hubbard, X. Wang, C.M. Agrawal (2000) Microstructural heterogeneity and the fracture toughness of bone. J Biomed Mater Res *51:* 735–745.
Pidaparti, R.M., D.B. Burr (1992) Collagen fiber orientation and geometry effects on the mechanical properties of secondary osteons. J Biomech *25:* 869–880.
Portigliatti Barbos, M., P. Bianco, A. Ascenzi (1983) Distribution of osteonic and interstitial components in the human femoral shaft with reference to structure, calcification and mechanical properties. Acta Anat *115:* 178–186.
Power, J., N. Loveridge, A. Lyon, N. Rushton, M. Parker, J. Reeve (2003) Bone remodeling at the endocortical surface of the human femoral neck: a mechanism for regional cortical thinning in cases of hip fracture. J Bone Miner Res *18:* 1775–1780.
Rauch, F., R. Travers, F.H. Glorieux (2007) Intracortical remodeling during human bone development – a histomorphometric study. Bone *40:* 274–280.
Reilly, G.C., J.D. Currey (1999) The development of microcracking and failure in bone depends on the loading mode to which it is adapted. J Exp Biol *202:* 543–552.
Reilly, G.C., J.D. Currey (2000) The effects of damage and microcracking on the impact strength of bone. J Biomech *33:* 337–343.
Reilly, G.C., J.D. Currey, A. Goodship (1997) Exercise of young thoroughbred horses increases impact strength of the third metacarpal bone. J Orthop Res *15:* 862–868.
Richman, E.A., D.J. Ortner, F.P. Schulter-Ellis (1979) Differences in intracortical bone remodeling in three aboriginal American populations: possible dietary factors. Calcif Tissue Int *28:* 209–214.
Robling, A.G., S.D. Stout (1999) Morphology of the drifting osteon. Cells Tissues Organs *164:* 192–204.
Rubin, C.T., L.E. Lanyon (1982) Limb mechanics as a function of speed and gait: a study of functional strains in the radius and tibia of horse and dog. J Exp Biol *101:* 187–211.
Rubin, C.T., L.E. Lanyon (1984) Regulation of bone formation by applied dynamic loads. J Bone Joint Surg Am *66:* 397–402.
Rubin, C.T., L.E. Lanyon (1985) Regulation of bone mass by mechanical strain magnitude. Calcif Tissue Int *37:* 411–417.
Saito, V.S. (1984) Pattern of osteons in the human femur diaphysis. Anat Anz Jena *55:* 297–301.
Schaffler, M.B., D.B. Burr (1984) Primate cortical bone microstructure: relationship to locomotion. Am J Phys Anthropol *65:* 191–197.
Schaffler, M. (2001) Bone fatigue and remodeling in the development of stress fractures; in Burr, D., C. Milgrom (eds): Musculoskeletal Fatigue and Stress Fractures. Boca Raton, CRC Press, pp 161–182.
Schneider, R.K., D.W. Milne, A.A. Gabel, J.J. Groom, L.R. Bramlage (1982) Multidirectional in vivo strain analysis of the equine radius and tibia during dynamic loading with and without a cast. Am J Vet Res *43:* 1541–1550.
Sinelnikov, N. (1937) On the disposition of the osteons in the diaphysis. Anthropol J *3:* 102–116.
Skedros, J.G. (1994) Collagen fiber orientation in skeletal tension/compression systems: a potential role of variant strain stimuli in the maintenance of cortical bone organization. J Bone Miner Res *9:* S251.
Skedros, J.G. (2001) Collagen fiber orientation: a characteristic of strain-mode-related regional adaptation in cortical bone. Bone *28:* S110–S111.
Skedros, J.G. (2005) Osteocyte lacuna population densities in sheep, elk and horse calcanei. Cells Tissues Organs *181:* 23–37.
Skedros, J.G., R.D. Bloebaum, K.N. Bachus, T.M. Boyce, B. Constantz (1993) Influence of mineral content and composition of graylevels in backscattered electron images of bone. J Biomed Mater Res *27:* 57–64.

Skedros, J.G., R.D. Bloebaum, M.W. Mason, D.M. Bramble (1994a) Analysis of a tension/compression skeletal system: possible strain-specific differences in the hierarchical organization of bone. Anat Rec *239:* 396–404.

Skedros, J.G., M.R. Dayton, C.L. Sybrowsky, R.D. Bloebaum, K. Bachus (2006a) The Influence of collagen fiber orientation and other histocompositional characteristics on the mechanical properties of equine cortical bone. J Exp Biol *209:* 3025–3042.

Skedros, J.G., T.R. Grunander, M.W. Hamrick (2005) Spatial distribution of osteocyte lacunae in equine radii and third metacarpals: considerations for cellular communication, microdamage detection and metabolism. Cells Tissues Organs *180:* 215–236.

Skedros, J.G., K.J. Hunt (2004) Does the degree of laminarity mediate site-specific differences in collagen fiber orientation in primary bone? An evaluation in the turkey ulna diaphysis. J Anat *205:* 121–134.

Skedros, J.G., K.J. Hunt, R.D. Bloebaum (2004) Relationships of loading history and structural and material characteristics of bone: development of the mule deer calcaneus. J Morphol *259:* 281–307.

Skedros, J.G., M.W. Mason, R.D. Bloebaum (1994b) Differences in osteonal micromorphology between tensile and compressive cortices of a bending skeletal system: indications of potential strain-specific differences in bone microstructure. Anat Rec *239:* 405–413.

Skedros, J.G., M.W. Mason, R.D. Bloebaum (2001) Modeling and remodeling in a developing artiodactyl calcaneus: a model for evaluating Frost's mechanostat hypothesis and its corollaries. Anat Rec *263:* 167–185.

Skedros, J.G., M.W. Mason, M.C. Nelson, R.D. Bloebaum (1996) Evidence of structural and material adaptation to specific strain features in cortical bone. Anat Rec *246:* 47–63.

Skedros, J.G., S.D. Mendenhall, W.E. Anderson, K.E. Gubler, J.V. Hoopes, S.M. Sorenson (2006b) Osteon phenotypic morphotypes: a new characteristic for interpreting bone quality in cortical bone. 52nd Annual Meeting of the Orthopaedic Research Society, Chicago, pp 1600.

Skedros, J.G., S.M. Sorenson, Y. Takano, C.H. Turner (2006c) Dissociation of mineral and collagen orientations may differentially adapt compact bone for regional loading environments: results from acoustic velocity measurements in deer calcanei. Bone *39:* 143–151.

Skedros, J.G., S.C. Su, R.D. Bloebaum (1997) Biomechanical implications of mineral content and microstructural variations in cortical bone of horse, elk, and sheep calcanei. Anat Rec *249:* 297–316.

Skedros, J.G., C.L. Sybrowsky, T.R. Parry, R.D. Bloebaum (2003) Regional differences in cortical bone organization and microdamage prevalence in Rocky Mountain mule deer. Anat Rec *274A:* 837–850.

Sobelman, O.S., J.C. Gibeling, S.M. Stover, S.J. Hazelwood, O.C. Yeh, D.R. Shelton, R.B. Martin (2004) Do microcracks decrease or increase fatigue resistance in cortical bone? J Biomech *37:* 1295–1303.

Sorenson, S.M., N.H. Jenson, J.G. Skedros (2004) Prevalence of atypical osteon characteristics may reflect adaptations in bending environments and during growth. J Bone Miner Res *19:* S223.

Stout, S.D., B.S. Brunsden, C.F. Hildebolt, P.K. Commean, K.E. Smith, N.C. Tappen (1999) Computer-assisted '3D' reconstruction of serial sections of cortical bone to determine the 3D structure of osteons. Calcif Tissue Int *65:* 280–284.

Stover, S.M., R.R. Pool, R.B. Martin, J.P. Morgan (1992) Histological features of the dorsal cortex of the third metacarpal bone mid-diaphysis during postnatal growth in thoroughbred horses. J Anat *181:* 455–469.

Su, S.C., J.G. Skedros, K.N. Bachus, R.D. Bloebaum (1999) Loading conditions and cortical bone construction of an artiodactyl calcaneus. J Exp Biol *202/22:* 3239–3254.

Swartz, S.M., M.B. Bennett, D.R. Carrier (1992) Wing bone stresses in free flying bats and the evolution of skeletal design for flight. Nature *359:* 726–729.

Szivek, J.A., E.M. Johnson, F.P. Magee (1992) In vivo strain analysis of the greyhound femoral diaphysis. J Invest Surg *5:* 91–108.

Takano, Y., C.H. Turner, I. Owan, R.B. Martin, S.T. Lau, M.R. Forwood, D.B. Burr (1999) Elastic anisotropy and collagen orientation of osteonal bone are dependent on the mechanical strain distribution. J Orthop Res *17:* 59–66.

Tappen, N.C. (1977) Three-dimensional studies of resorption spaces and developing osteons. Am J Anat *149:* 301–332.

Turner, A.S., E.J. Mills, A.A. Gabel (1975) In vivo measurement of bone strain in the horse. Am J Vet Res *36:* 1573–1579.

Turner, C.H., D.B. Burr (1993) Basic biomechanical measurements of bone: a tutorial. Bone *14:* 595–608.

Ural, A., D. Vashishth (2006) Cohesive finite element modeling of age-related toughness loss in human cortical bone. J Biomech *39:* 2974–2982.

Urbanová, P., V. Novotný (2005) Distinguishing between human and non-human bones: histometric method for forensic anthropology. Anthroplogie *XLIII:* 77–85.

Vajda, E.G. (1998) Age-Related Changes in the Microstructure and Mineralization of the Female Proximal Femur; PhD dissertation, University of Utah, Salt Lake City, p 210.

Vajda, E.G., R.D. Bloebaum (1999) Age-related hypermineralization in the female proximal human femur. Anat Rec *255:* 202–211.

Vashishth, D. (2004) Rising crack-growth-resistance behavior in cortical bone: implications for toughness measurements. J Biomech *37:* 943–946.

Vashishth, D., J. Koontz, S.J. Qiu, D. Lundin-Cannon, Y.N. Yeni, M.B. Schaffler, D.P. Fyhrie (2000) In vivo diffuse damage in human vertebral trabecular bone. Bone *26:* 147–152.

Weidmann, S.M. (1956) The renewal of inorganic phosphate in bones of various species of small mammal as a function of time. Biochem J *62:* 593–601.

Zioupos, P., J.D. Currey (1998) Changes in the stiffness, strength, and toughness of human cortical bone with age. Bone *22:* 57–66.